Electronic Supplementary Information (ESI) for

Linear π-Conjugated Polycyclic Compounds Consisting of Four-, Five-, and Six-Membered Rings: Benzo[1”,2”:3,4;4”,5”:3’,4’]bis(cyclobuta[1,2-*c*]thiophene)

Tatsuru Kuroiwa, Daisuke Asai, Shingo Hashimoto, and Kazukuni Tahara*

Department of Applied Chemistry, School of Science and Technology, Meiji University, 1-1-1 Higashimita, Tama-ku, Kawasaki, Kanagawa, 214-8571, Japan.

This file includes:

1. Synthesis

1-1. General Methods

THF was passed through activated alumina and copper catalysts in a Glass Contour solvent purification system. Toluene was distilled before use. Dehydrated Et_2O and 1,4-dioxane were purchased from FUJIFILM Wako Chemicals. Other commercially available reagents were used as received. $Pd(PPh_3)_4$ was prepared following the reported procedure.[1]

^1H (500 or 400 MHz) and ^{13}C (125 or 100 MHz) NMR spectra were measured on a JEOL ECA500, ECA400, or JNM-ECZ400S spectrometer. When chloroform-*d* was used as the solvent, the NMR spectra were referenced to a tetramethylsilane signal in the ^1H and ^{13}C NMR spectra (0.00 ppm). When acetone-d_6, benzene-d_6, and dichloromethane-d_2 were used as the solvents, the ^1H NMR spectra were referenced to residual solvent signals (2.05, 7.16, and 5.32 ppm). The ^{13}C NMR spectra in dichloromethane-d_2 were referenced to a residual solvent signal (53.84 ppm). Recycling HPLC separation was undertaken with a JAI LC-5060 recycling chromatograph using 600 mm × 20 mm JAIGEL-1HR and 2HR GPC columns with $CHCl_3$ or CH_2Cl_2 as the eluent. Other spectra were recorded using the following instruments: IR spectra, JACSCO FT/IR-410; mass spectra, JMS-T100GCV (TOF); melting point (m.p.), Stuart Scientific SMP3. Oil baths (Fine, FGO-180D) and UT-106H (SHARP) were used as the heat and ultrasonic sources in the following procedures.

Scheme S1. Synthesis of biphenylene.

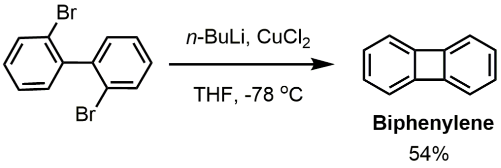

Synthesis of Biphenylene. Under argon atmosphere, 2,2'-dibromobiphenyl (250 mg, 802 μmol) and THF (16.9 mL) were added to a dried two-necked flask (50 mL). *n*-BuLi (1.18 mL, 1.8 mmol, 1.5 M in *n*-hexane) was added dropwise to the mixture at −78 °C. After being stirred at −78 °C for 75 min, dried $CuCl_2$ (332 mg, 2.47 mmol) was added to the mixture in one portion. The resulting mixture was allowed to warm naturally to room temperature with continuous stirring overnight. The reaction was quenched by the addition of NH_4Cl aq., and the products were extracted with ethyl acetate. The organic phase was washed with water and brine, and dried over $MgSO_4$. After evaporation of the solvents, the residue was subjected to the silica gel column chromatography (hexane) and recycling HPLC separations ($CHCl_3$) to give biphenylene as a white solid (65.4 mg, 54% yield). The ^{1}H spectrum of biphenylene in $CDCl_3$ agreed with that in a previous report.[2] ^{1}H NMR (500 MHz, $CDCl_3$, 25 °C) δ 6.77–6.69 (m, 4H), 6.66–6.59 (m, 4H).

Scheme S2. Synthesis of ***c*BCT**.

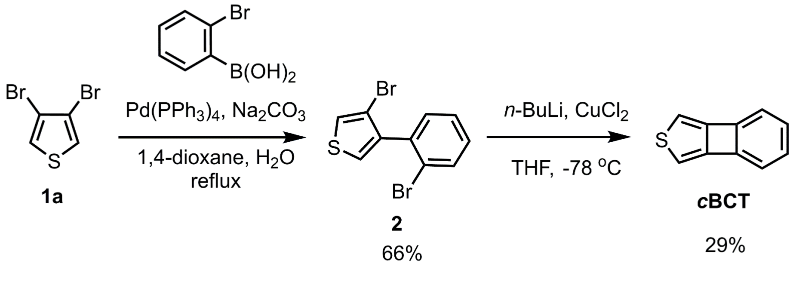

Synthesis of 3-Bromo-4-(2-bromophenyl)thiophene (2). Under argon atmosphere, 3,4-dibromothiophene (**1a**, 1.30 mL, 11.9 mmol), (2-bromophenyl)boronic acid (1.58 g, 7.87 mmol), $Pd(PPh_3)_4$ (744 mg, 644 μmol), and Na_2CO_3 (1.63 g, 15.4 mmol) were added to a Schlenk tube (200 mL). Then, 1,4-dioxane (16.0 mL) and H_2O (5.0 mL) were added to the mixture. The mixture was refluxed for 6 d. After cooling naturally down to room temperature, the products were extracted with *t*BuOMe. The organic phase was washed with water and brine, and dried over $MgSO_4$. After evaporation of the solvents, the residue was subjected to the column chromatography on silica gel (hexane). Compound **2** was obtained as colorless oil (1.65 g, 66% yield). The ^{1}H NMR spectrum of **2** in $CDCl_3$ agreed with that in a previous report.[3] ^{1}H NMR (500 MHz, $CDCl_3$, 26 °C) δ 7.67 (d, J = 8.0 Hz, 1H), 7.39−7.33 (m, 2H), 7.32−7.22 (m, 3H).

Synthesis of Benzo[3,4]cyclobuta[1,2-*c*]thiophene (*c*BCT). Under argon atmosphere, 3-bromo-4-(2-bromophenyl)thiophene (**2**, 619 mg, 1.95 mmol) and THF (40.4 mL) were added to a dried Schlenk tube (200 mL). *n*-BuLi (3.11 mL, 4.7 mmol, 1.5 M in *n*-hexane) was added dropwise at −78 °C. After being stirred at −78 °C for 1 h, dried $CuCl_2$ (807 mg, 6.00 mmol) was added to the mixture in one portion. After being stirred at −78 °C for 1 h, the resulting mixture was allowed to warm naturally to room temperature with continuous stirring overnight. The reaction was quenched by the addition of NH_4Cl aq., and the products were extracted with ethyl acetate. The organic phase was washed with water and brine, and dried over $MgSO_4$. After evaporation of the solvents, the residue was subjected to the silica gel column chromatography (hexane) and recycling HPLC separations ($CHCl_3$) to give ***c*BCT** as a white solid (88.3 mg, 29% yield). The ^{1}H and ^{13}C NMR spectra of ***c*BCT** in $CDCl_3$ agreed with those in previous reports.[4,5] ^{1}H NMR (500 MHz, $CDCl_3$, 26 °C) δ 6.95−6.90 (m, 2H), 6.89−6.83 (m, 2H), 6.53 (s, 2H); ^{1}H NMR (500 MHz, acetone-d_6, 25 °C) δ 7.02–6.90 (m, 4H), 6.75 (s, 2H); $^{13}C\{^1H\}$ NMR (126 MHz, $CDCl_3$, 25 °C) δ 146.6, 145.5, 128.4, 118.1, 112.6.

Scheme S3. Synthesis of Compound **3**.

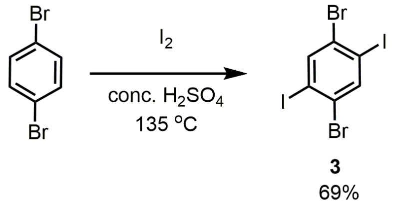

Synthesis of 1,2-Dibromo-2,5-diiodobenzene (3). 1,4-Dibromobenzene (15.0 g, 63.6 mmol), iodine (35.4 g, 139 mmol), and conc. H_2SO_4 (120 mL) were added to a round-bottom flask (300 mL) equipped with a reflux condenser. The mixture was stirred at 135 °C for 40 h. After naturally cooling the mixture to room temperature, the mixture was poured into ice-cold water. The precipitate was collected by filtration. The solid materials left at the bottom of the flask were also collected. The combined solid materials were dissolved in $CHCl_3$, and the product was recrystallized by the addition of MeOH. Compound **3** was isolated as a white solid (21.3 g, 69% yield). The ^1H NMR spectrum of **3** in $CDCl_3$ agreed with that in a previous report.[6] ^1H NMR (500 MHz, $CDCl_3$, 25 °C) δ 8.05 (s, 2H).

Scheme S4. Synthesis of **BBCT**.

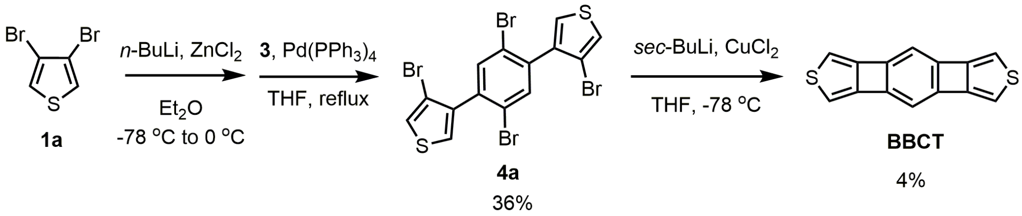

Synthesis of 1,4-Dibromo-2,5-bis(4-bromothiophen-3-yl)benzene (4a). Under argon atmosphere, 3,4-dibromothiophene (**1a**, 0.660 mL, 6.00 mmol) and dehydrated Et_2O (6.0 mL) were added to a dried two-necked flask (100 mL) equipped with a reflux condenser. To the mixture with continuous stirring at −78 °C, *n*-BuLi (3.95 mL, 5.9 mmol, 1.5 M in *n*-hexane) was added dropwise over 5 min. After being stirred at −78 °C for 1 h, a solution of $ZnCl_2$ (3.0 mL, 6.0 mmol, 2.0 M in 2-methyltetrahydrofuran) was added. The mixture was further stirred for 1 h at 0 °C. 1,4-Dibromo-2,5-

diiodobenzene (**3**, 975 mg, 2.00 mmol), $Pd(PPh_3)_4$ (43.6 mg, 37.7 μmol), and THF (18 mL) were added to the mixture. After being stirred at 75 °C for 18 h, the reaction was terminated by the addition of NH_4Cl aq. The products were extracted with ethyl acetate. The organic phase was washed with brine, and dried over $MgSO_4$. After evaporation of the solvents, CH_2Cl_2 was added to the crude mixture, and the supernatant was removed from the suspension. After repeating this washing treatment twice, toluene and EtOH were added, and the ultrasonic was irradiated to the mixture. The resulting solid materials were filtered and washed with hexane. The compound **4a** was obtained as a white solid (406 mg, 36% yield). m.p. 203.1–203.7 °C; ^1H NMR (500 MHz, $CDCl_3$, 25 °C) δ 7.61 (s, 2H), 7.39 (d, J = 3.5 Hz, 2H), 7.35 (d, J = 3.5 Hz, 2H); $^{13}C\{^1H\}$ NMR (126 MHz, $CDCl_3$, 25 °C) δ 139.6, 137.8, 135.4, 125.5, 123.6, 122.7, 111.9; IR (KBr) 3115, 3093, 1766, 1603, 1538, 1458, 1406, 1389, 1358, 1304, 1207, 1096, 1050, 919, 887, 856, 797, 732, 722, 669, 640 cm^{-1}; HRMS (FD) *m/z* calcd for $C_{14}H_6{}^{79}Br_4S_2$ (M^+): 553.6644, found 553.6629.

Synthesis of Benzo[1”,2”:3,4;4”,5”:3’,4’]bis(cyclobuta[1,2-*c*])thiophene (BBCT). Under argon atmosphere, THF (50.0 mL) was added to a dried Schlenk tube (200 mL). To the mixture at −78 °C, *sec*-BuLi (9.0 mL, 11 mmol, 1.23 M in cyclohexane) was added dropwise. After being stirred at −78 °C for 17 min, compound **4a** (837 mg, 1.50 mmol) was added over 3 min. To the mixture being stirred at −78 °C for 22 min, dried $CuCl_2$ (2.12 g, 15.8 mmol) was added in one portion. The resulting mixture was allowed to warm naturally to room temperature. The reaction was quenched with NH_4Cl aq., and the products were extracted with ethyl acetate. The organic phase was washed with water and brine, and dried over $MgSO_4$. The solvents were removed under vacuum. The residue was subjected to the column chromatography on silica gel (hexane/toluene = 4/1). Further purification by the recrystallization from MeOH and recycling HPLC separation (CH_2Cl_2) gave **BBCT** as a yellow solid (13.0 mg, 4%). m.p. over 260 °C (decomposed); ^1H NMR (500 MHz, CD_2Cl_2, 25 °C) δ 6.60 (s, 2H), 6.45 (s, 4H); ^1H NMR (500 MHz, acetone-d_6, 25 °C) δ 6.73 (s, 2H), 6.65 (s, 4H); $^{13}C\{^1H\}$ NMR (126

MHz, CD_2Cl_2, 25 °C) δ 147.2, 145.4, 112.2, 111.2; IR (KBr) 3089, 1767, 1618, 1563, 1521, 1294, 1248, 1143, 1078, 878, 855, 785, 767, 731 cm^{-1}; HRMS (FD) *m/z* calcd for $C_{14}H_6S_2$ (M^+): 237.9911, found 237.9900.

Scheme S5. Synthesis of **BBCT-Me**.

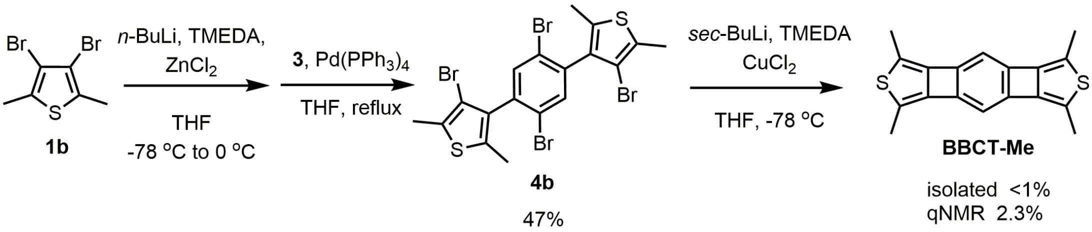

Synthesis of 4b. Under argon atmosphere, 3,4-dibromo-2,5-dimethylthiophene (**1b**, 5.76 g, 21.3 mmol), THF (42.6 mL), and *N,N,N',N'*-tetramethylethylenediamine (TMEDA, 3.18 mL, 21.3 mmol) were added to a dried two-necked flask (300 mL) equipped with a reflux condenser. *n*-BuLi (3.95 mL, 5.9 mmol, 1.5 M in *n*-hexane) was added dropwise over 10 min to the mixture at −78 °C. After being stirred at −78 °C for 1 h, a solution of $ZnCl_2$ (11 mL, 22 mmol, 2.0 M in 2-methyltetrahydrofuran) was added. The mixture was stirred at 0 °C for 1 h, and then 1,4-dibromo-2,5-diiodobenzene (**3**, 3.46 g, 7.09 mmol), $Pd(PPh_3)_4$ (348 mg, 301 μmol), and THF (21.3 mL) were added. The mixture was continuously stirred at 75 °C for 22 h. The reaction was quenched with NH_4Cl aq., and the products were extracted with ethyl acetate. The organic phase was washed with brine, and dried over $MgSO_4$. After evaporation of the solvents, the residue was subjected to the silica gel column chromatography (hexane). After evaporation of the solvents, toluene and EtOH were added to the mixture. The solid materials were filtered and washed with acetone to give **4b** as a white solid (2.04 g, 47%). The characterization was performed for the inseparable mixture of two stereoisomers. m.p. 235.4–236.0 °C; ^{1}H NMR (500 MHz, $CDCl_3$, 25 °C) δ 7.49 (s, 2H), 2.41 (s, 6H), 2.29–2.24 (m, 6H); $^{13}C\{^1H\}$ NMR (126 MHz, $CDCl_3$, 25 °C) δ 138.4, 136.3, 136.2, 135.5, 134.1, 133.8, 130.8, 123.4, 110.3, 110.1, 15.0, 14.5; IR (KBr) 2917, 2852, 1772, 1567, 1507, 1436, 1362, 1296, 1201, 1144, 1068, 1028, 995, 896, 845, 778, 757, 743 cm^{-1}; HRMS (FD) *m/z* calcd for $C_{18}H_{14}{}^{79}Br_4S_2$ (M^+): 609.7270, found 609.7290.

Synthesis of BBCT-Me. Under argon atmosphere, THF (60.0 mL) and TMEDA (2.98 mL, 20.0 mmol) were added to a dried Schlenk tube (200 mL). *sec*-BuLi (13.0 mL, 16 mmol, 1.23 M in cyclohexane) was added dropwise to the mixture at −78 °C. After being stirred at −78 °C for 40 min, 1,4-dibromo-2,5-bis(4-bromo-2,5-dimethylthiophen-3-yl)benzene (**4b**, 1.22 g, 2.00 mmol) was added over 3 min. After being stirred at −78 °C for 26 min, dried $CuCl_2$ (2.46 g, 18.3 mmol) was added in one portion to the mixture at −78 °C. The resulting mixture was stirred at −78 °C for 40 min, and then allowed to warm naturally to room temperature. After being stirred for 2 h, the reaction was terminated with brine and the products were extracted with toluene. The organic phase was washed with brine, and dried over Na_2SO_4. The solvents were removed under vacuum. The residue was subjected to the column chromatography on silica gel (hexane/Et_3N = 100/1) and recycling HPLC separation (CH_2Cl_2). Recrystallization from toluene afforded **BBCT-Me** as a yellow solid (4.9 mg, 0.8%). m.p. over 275 °C (decomposed); ^{1}H NMR (500 MHz, CD_2Cl_2, 25 °C) δ 6.52 (s, 2H), 2.17 (s, 12H); ^{1}H NMR (500 MHz, acetone-d_6, 25 °C) δ 6.70 (s, 2H), 2.16 (s, 12H); $^{13}C\{^1H\}$ NMR (126 MHz, CD_2Cl_2, 25 °C) δ 145.8, 140.6, 125.7, 110.3, 13.4; IR (KBr) 3058, 2965, 2912, 2848, 1731, 1672, 1428, 1372, 1287, 1237, 1184, 1168, 1126, 863, 737 cm^{-1}; HRMS (FD) *m/z* calcd for $C_{18}H_{14}S_2$ (M^+): 294.0537, found 294.0528.

Scheme S6. Synthesis of [3]phenylene.

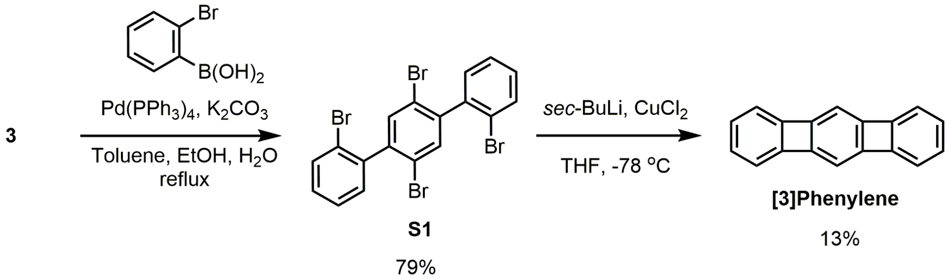

Synthesis of 2,2',2",5'-Tetrabromo-1,1':4',1"-terphenyl (S1). Under argon atmosphere, 1,4-dibromo-2,5-diiodobenzene (**3**, 1.95 g, 4.00 mmol), (2-bromophenyl)boronic acid (1.94 g, 9.66 mmol), $Pd(PPh_3)_4$ (144 mg, 125 μmol), and K_2CO_3 (3.36 g, 24.3 mmol) were added to a two-necked flask (200 mL) equipped with a reflux condenser. Toluene (32 mL), EtOH (10 mL), and H_2O (15 mL) were added to the mixture. After being stirred at 90 °C for 8 h, (2-bromophenyl)boronic acid (485 mg, 2.42 mmol) was added. Further stirring at 90 °C for 13 h, the mixture was naturally cooled to room temperature. The products were extracted with CH_2Cl_2. The organic phase was washed with water and brine, and dried over $MgSO_4$. When the solvents were evaporated to a small volume, the precipitate was generated. The precipitate was collected by filtration and washed with hexane. Compound **S1** was isolated as a white solid (1.72 g, 79%). The ^{1}H NMR spectrum of **S1** agreed with that in a previous report.[7] ^{1}H NMR (500 MHz, acetone-*d*$_6$, 25 °C) δ 7.78 (dd, *J* = 8.0 Hz, 1.0 Hz, 2H), 7.67 (s, 1H), 7.64 (s, 1H), 7.57–7.50 (m, 2H), 7.46–7.38 (m, 4H).

Synthesis of [3]Phenylene. Under argon atmosphere, THF (50.0 mL) was added to a dried Schlenk tube (200 mL). After the addition of *sec*-BuLi (11.0 mL, 13.5 mmol, 1.23 M in cyclohexane) at –78 °C, 2,2',2",5'-tetrabromo-1,1':4,'1"-terphenyl (**S1**, 765 mg, 1.40 mmol) was added over 3 min to the mixture at –78 °C. After being stirred at −78 °C for 30 min, dried $CuCl_2$ (1.93 g, 14.4 mmol) was added to the mixture in one portion. The reaction mixture was allowed to warm naturally to room temperature with continues stirring overnight. The reaction was terminated by the addition of brine. The products were extracted with toluene. The organic phase was washed with water and brine, and dried over $MgSO_4$. After removal of the solvents under vacuum, hexane was added to the crude mixture. Insoluble solid material was washed with hexane, and the supernatant was removed from the suspension. After repeating this treatment twice, the residue was recrystallized from toluene. Additional purification by recycling HPLC separation ($CHCl_3$) gave [3]phenylene as a red solid (42.6 mg, 13%). The ^{1}H NMR spectrum of [3]phenylene in benzene-d_6 agreed with that in a previous report.[2] ^{1}H NMR (500 MHz, benzene-d_6, 25 °C) δ 6.49–6.41 (m, 4H), 6.23–6.16 (m, 4H), 5.93 (s, 2H); ^{1}H NMR (500 MHz, acetone-d_6, 25 °C) δ 6.69–6.63 (m, 4H), 6.52–6.46 (m, 4H), 6.41 (s, 2H).

2. Additional Information of the UV-vis Absorption Spectra

Table S1. The absorption maxima and molar absorbabilities of **BBCT**, **BBCT-Me**, ***c*BCT**, and [3]phenylene.

compound	wavelength (nm)	$\varepsilon \times 10^4$ ($L \cdot mol^{-1} \cdot cm^{-1}$)
BBCT	423	3.00
	403	1.80
	285	5.65
	217	1.64
BBCT-Me	427	2.76
	406	1.83
	304	5.35
	260	2.09
***c*BCT**	348	1.13
	331	0.97
	249	4.48
[3]phenylene	433	2.98
	408	1.76
	287	10.26
	276	7.21

3. Electrochemical Measurements

The electrochemical measurements were performed on a HOKUTO DENKO HZ-7000 voltammetric analyzer under an argon atmosphere. The counter electrode was a platinum wire, the working electrode was glassy carbon, and the reference electrode was an Ag/Ag$^+$ electrode, respectively. The CH_2Cl_2 was degassed by argon prior to use. Recrystallized [*n*-Bu_4N][ClO_4] from hot EtOH was used as the supporting electrolyte. Ferrocene purified by sublimation was used as an internal standard. Cyclic voltammetry (CV) mode at a scan rate of 100 mV/s was used. The potential (V) was corrected against the ferrocene/ferrocenium (Fc/Fc$^+$) redox couple.

We estimated the half-wave potential of the Fc/Fc$^+$ redox couple $E_{1/2}$ (Fc/Fc$^+$) using the following equation.[8,9]

$$E_{1/2}\ (\mathrm{Fc/Fc^+}) = (E_{\mathrm{ap}} + E_{\mathrm{cp}})/2$$

E_{ap} and E_{cp} represent the anodic and cathodic peak potentials, respectively. In our electrochemical setup, E_{ap} and E_{cp} values are 0.50 V and −0.08 V, 0.53 V and −0.01 V, 0.30 V and 0.10 V, and 0.38 V and 0.07 V for **BBCT**, **BBCT-Me**, ***c*BCT**, and [3]phenylene, respectively. The $E_{1/2}$ (Fc/Fc$^+$) values are 0.29 V, 0.27 V, 0.10 V, and 0.16 V relative to the Ag/Ag$^+$ reference electrode, respectively. The voltammograms were then calibrated based on these $E_{1/2}$ (Fc/Fc$^+$) values.

Based on the energy level of the ferrocene/ferrocenium (Fc/Fc$^+$) couple (–4.8 eV) in vacuum,[8,9] we estimated the HOMO energy levels of the molecules using the following equation.

$$E_{\mathrm{HOMO}} = -(4.8 + E_{\mathrm{oxi,onset}})\ \mathrm{eV}$$

$E_{\mathrm{oxi,onset}}$ is the onset potential of the first oxidation wave relative to the Fc/Fc$^+$ couple. The calculated E_{HOMO} values are –5.2 eV and –5.0 eV for **BBCT** and **BBCT-Me**, respectively.

4. Computational Details

4–1. General

All quantum chemical calculations were performed using the Gaussian 16 program package (Revision A.03) under vacuum unless otherwise noted.[10] All molecular geometries were optimized at B3LYP[11–13]/6-311+G(d,p)[14–16] level of theory at the singlet ground state. Note that this basis set level is higher than that used in our previous work.[17] Vibrational-frequency calculations confirmed the absence of imaginary frequencies for all optimized geometries. All molecules adopt planar geometries with a D_{2h} symmetry group, except for ***c*BCT** (C_{2v} symmetry group).

4–2. Energy Estimation of the 4MR Formation

We estimated the energies of the 4MR formation using the zero-point-corrected total energies of simple model compounds. All molecules are optimized by DFT calculations at B3LYP/6-311+G(d,p) level of theory. There is a very small energy difference (0.4 kcal/mol) in the C–C bond formation of biphenyl from two benzene molecules and of phenylthiophene from benzene and thiophene molecules (Figure S1). The energies of the single 4MR formation are estimated to be 55.0 kcal/mol and 59.9 kcal/mol for biphenylene and ***c*BCT**, respectively (Figures S1a,b). Those of the double 4MR formation are 109 kcal/mol and 118 kcal/mol for [3]phenylene and **BBCT**, respectively (Figures S1c,d). The 4MR formation between the thiophene and benzene rings needs an additional energy cost compared with that between the benzene rings. This indicates larger strain energies of the 4MRs in ***c*BCT** and **BBCT**.

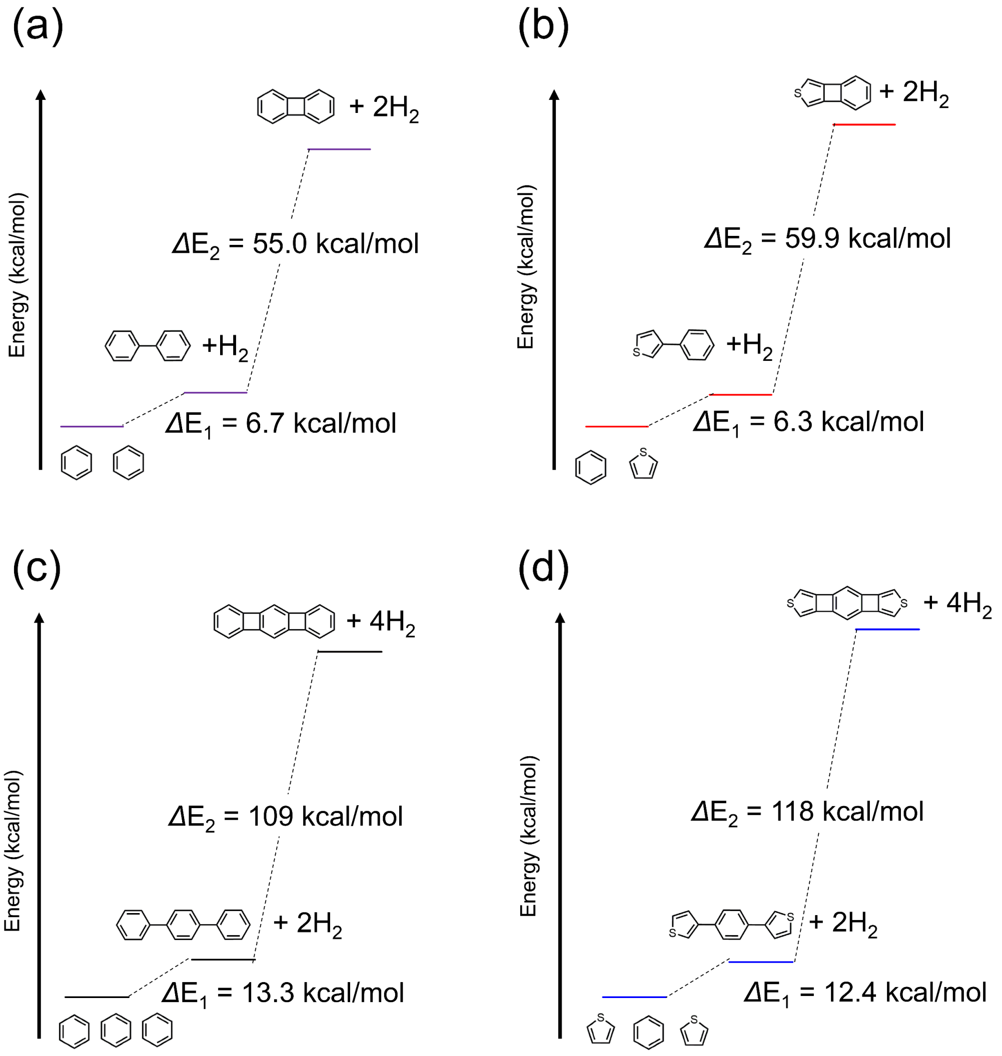

Figure S1. Energetics of the single (a, b) and double 4MR formation (c, d) estimated by the DFT calculations of the model compounds. The chemical structures of the model compounds are shown in each panel. The energies of the C-C single bond formation are also included.

4–3. TD-DFT Calculations of BBCTs, *c*BCT, and [3]Phenylene

Time-dependent DFT (TD-DFT) calculations at the B3LYP/6-311+G(d,p) level of theory were newly performed using the optimized structures calculated at a singlet ground state, in order to estimate excited state energies. The electronic transitions of each molecule are summarized in Tables S2–S5, and simulated UV-vis spectra are shown in Figure S2. Only in the case of **BBCT-Me**, the energetical order of the LUMO and LUMO+1 was swapped between the optimized geometries at the singlet ground (S_0) and excited states (S_1). The low energy transition (excite state 1) for [3]phenylene is attributed to its lowered HOMO energy level.

Table S2. Major electronic transitions of **BBCT**.

excited state	wavelength (nm)	oscillation strength (*f*)	major contributions
1	446.20	0.0066	61 (HOMO) -> 62 (LUMO, 70%)
2	388.90	0.4630	60 -> 62 (-25%), 61 -> 63 (66%)
3	298.02	0.0000	59 -> 62 (69%), 61 -> 69 (14%)
4	278.93	0.0000	59 -> 66 (-13%), 61 -> 64 (69%)
5	278.43	0.0000	58 -> 62 (53%), 59 -> 63 (-31%), 61 -> 65 (-34%)
6	276.69	0.0000	59 -> 64 (-13%), 61 -> 66 (69%)
7	273.47	1.2515	60 -> 62 (66%), 61 -> 63 (24%)
8	273.15	0.0074	60 -> 63 (70%)
9	270.71	0.0000	59 -> 63 (56%), 61 -> 65 (-43%)
10	266.40	0.0000	61 -> 67 (70%)

Table S3. Major electronic transitions of **BBCT-Me**.

excited state	wavelength (nm)	oscillation strength (*f*)	major contributions
1	432.46	0.0127	77 (HOMO) -> 79 (70%)
2	396.07	0.4366	76 -> 79 (-26%), 77 -> 78 (LUMO, 65%)
3	296.49	0.0340	76 -> 78 (70%)
4	294.68	0.0000	74 -> 82 (-13%), 77 -> 80 (68%), 77 -> 85 (-13%)
5	294.25	0.0000	74 -> 79 (69%), 77 -> 89 (-13%)
6	292.58	0.0000	74 -> 80 (-12%), 77 -> 82 (68%)
7	291.00	1.3579	76 -> 79 (65%), 77 -> 78 (26%)
8	290.35	0.0000	74 -> 78 (-27%), 75 -> 79 (58%), 77 -> 84 (-29%)
9	284.72	0.0000	77 -> 81 (70%)
10	271.12	0.0000	74 -> 78 (58%), 77 -> 84 (-38%)

Table S4. Major electronic transitions of ***c*BCT**.

excited state	wavelength (nm)	oscillation strength (*f*)	major contributions
1	333.01	0.0062	41 (HOMO) -> 43 (70%)
2	315.11	0.1676	40 -> 43 (-31%), 41 -> 42 (LUMO, 63%)
3	257.70	0.0000	41 -> 44 (69%)
4	248.23	0.0035	40 -> 42 (70%)
5	241.56	0.0003	41 -> 45 (70%)
6	238.03	0.6968	39 -> 43 (-18%), 40 -> 43 (60%), 41 -> 42 (28%), 41 -> 48 (15%)
7	226.90	0.2270	38 -> 42 (19%), 39 -> 43 (49%), 40 -> 43 (16%), 41 -> 42 (14%), 41 -> 48 (-41%)
8	225.94	0.0121	41 -> 46 (70%)
9	216.33	0.0000	41 -> 47 (68%), 41 -> 50 (-12%)
10	215.72	0.0058	39 -> 44 (-12%), 40 -> 44 (67%), 41 -> 49 (10%)

Table S5. Major electronic transitions of [3]phenylene.

excited state	wavelength (nm)	oscillation strength (*f*)	major contributions
1	549.84	0.0001	59 (HOMO) -> 60 (LUMO, 71%)
2	393.51	0.3930	57 -> 60 (26%), 59 -> 61 (65%)
3	339.32	0.0000	58 -> 60 (13%), 59 -> 62 (69%)
4	309.88	0.0000	58 -> 60 (69%), 59 -> 62 (-13%)
5	289.93	0.0000	56 -> 60 (-47%), 57 -> 62 (13%), 58 -> 61 (16%), 59 -> 63 (49%)
6	277.33	1.3779	57 -> 60 (65%), 59 -> 61 (-25%)
7	274.58	0.0000	59 -> 64 (70%)
8	265.22	0.0000	56 -> 60 (-20%), 58 -> 61 (56%), 59 -> 63 (-38%)
9	260.71	0.0028	59 -> 65 (70%)
10	255.49	0.0000	59 -> 66 (70%)

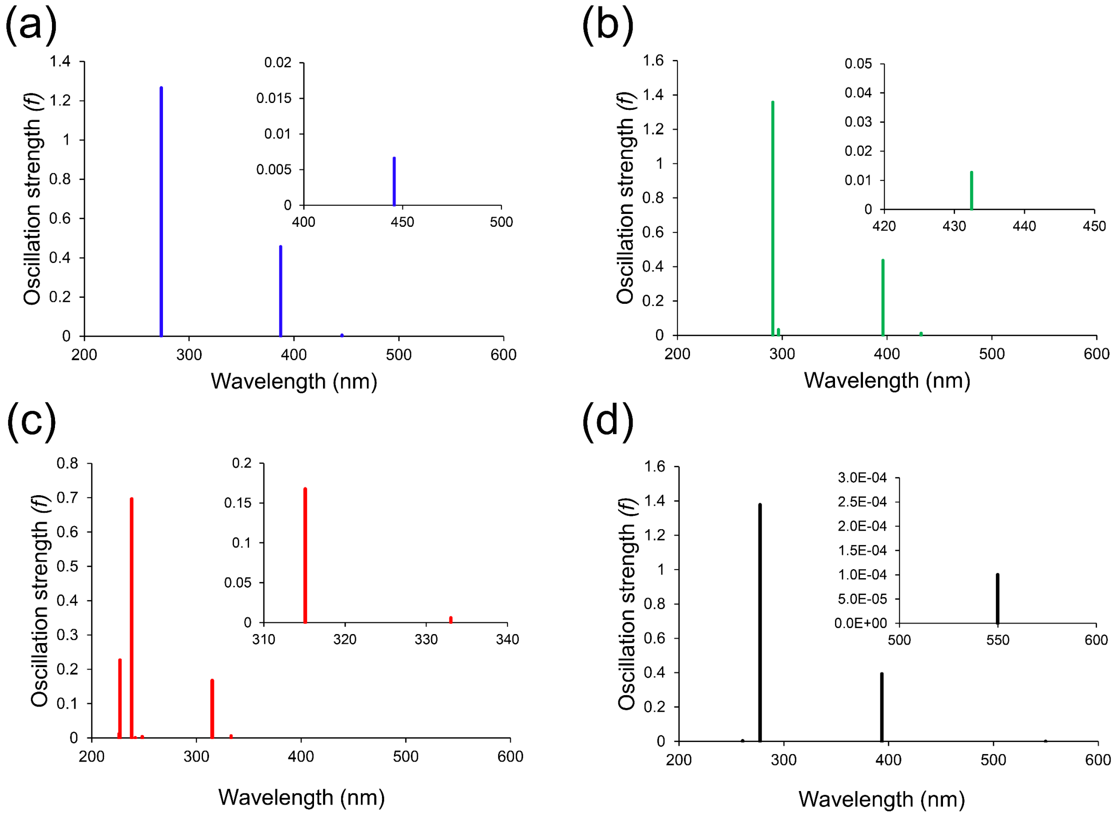

Figure S2. Predicted UV-vis spectra of (a) **BBCT**, (b) **BBCT-Me**, (c) ***c*BCT**, and (d) [3]phenylene by the TD-DFT calculations.

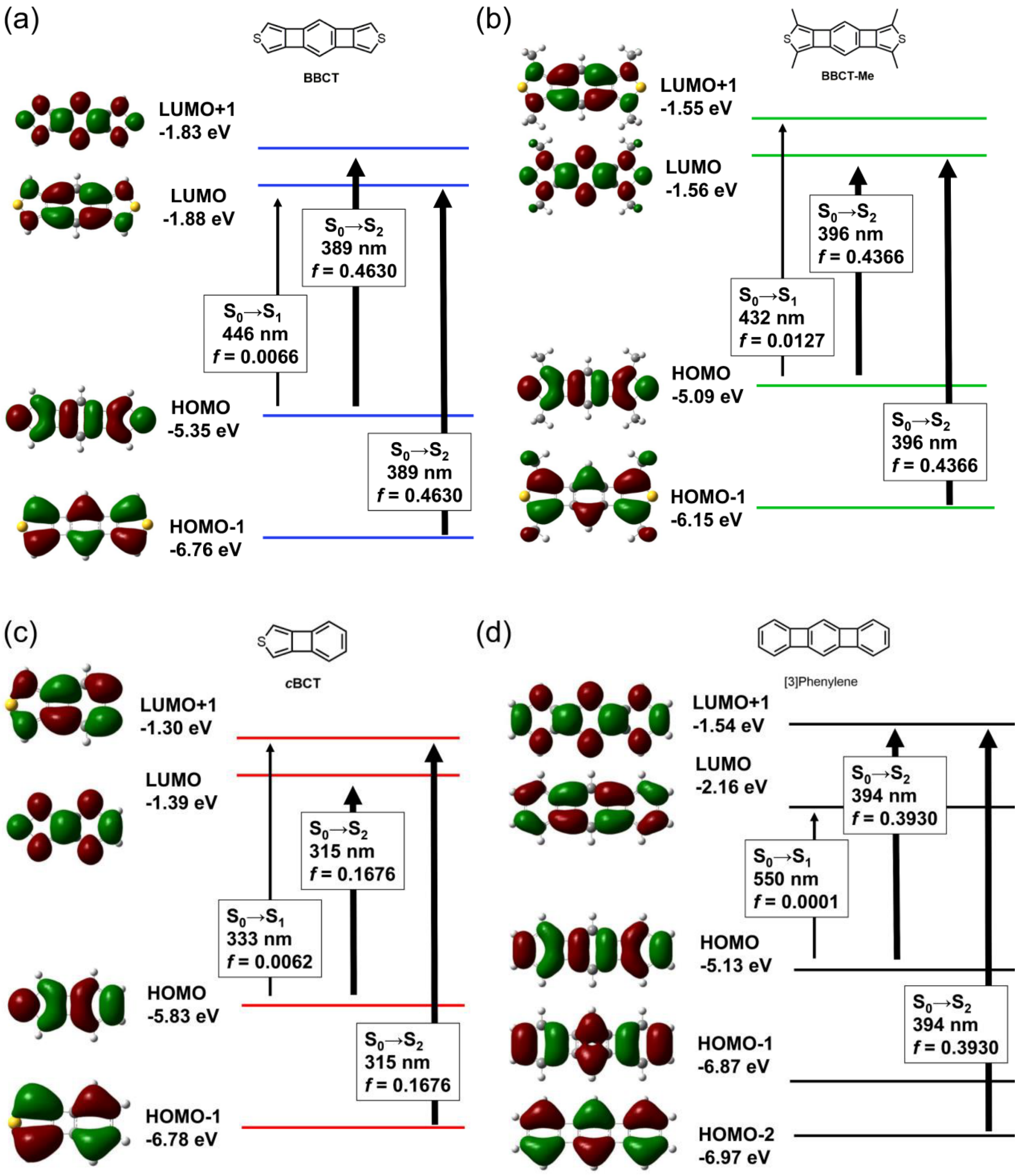

Figure S3. Major low energy transitions of **BBCT** (a), **BBCT-Me** (b), ***c*BCT** (c), and [3]phenylene (d) predicted by the TD-DFT calculations. Energy levels and distribution of the HOMO–1, HOMO, LUMO, and LUMO+1 of the optimized molecules at a singlet ground state (S_0) are also shown in each panel.

4–5. NICS Analysis

The calculations of nucleus-independent chemical shift (NICS)[18] were performed for the optimized geometry of **BBCT-Me** at B3LYP/6-311+G(d,p) level of theory using the gauge-independent atomic orbital (GIAO) method (Figure S4a).[19] In this study, we used NICS(1)$_{zz}$ values which are the zz component of the isotropic NICS values calculated at 1 Å above the ring centers (NICS(1)$_{iso}$).[20] It should be noted that the NICS(1)$_{zz}$ analysis gives more reliable results for magnetic response compared with the NICS(1)$_{iso}$ or NICS(0)$_{iso}$ analysis in the case of planar molecular systems. NICS-XY scans[21–23] were also performed with the aid of the Aroma program (Figure S4b).[24] The ghost atoms (BQs) were placed at step intervals of 0.1 Å. As the NICS scan of ***c*BCT** was reported previously,[17] we here performed the NICS scans of **BBCT**, **BBCT-Me**, and [3]phenylene.

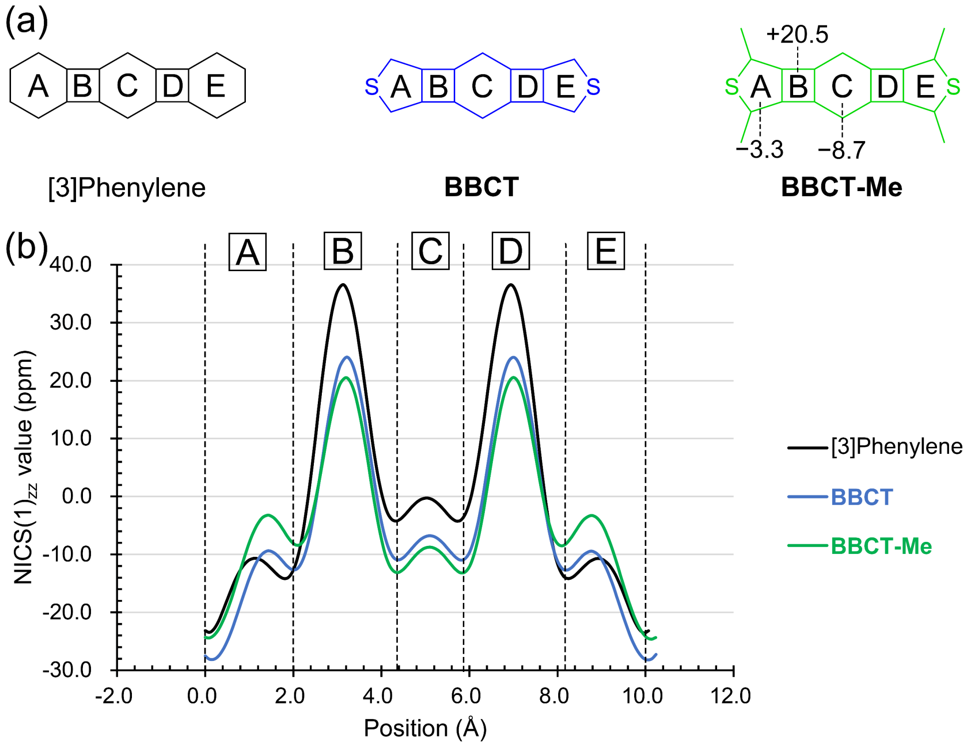

Figure S4. (a) Ring labels of [3]phenylene, **BBCT**, and **BBCT-Me**, and the calculated NICS(1)$_{zz}$ values (ppm) at each ring center of **BBCT-Me**. (b) The results of NICS-XY scan analyses for [3]phenylene (black), **BBCT** (blue), and **BBCT-Me** (green).

4–6. GIMIC Calculations

In our previous work, the current flows and strengths of the bonds only at the periphery of [3]phenylene, ***c*BCT**, and **BBCT** were reported.[17] We performed the gauge-including magnetically induced current (GIMIC) calculations for [3]phenylene, ***c*BCT**, **BBCT**, and **BBCT-Me** to estimate the strengths and paths of magnetically induced currents at all bonds (Figure S5).[25–27] Prior to the GIMIC calculations, atomic orbital density matrices, first-order perturbed atomic orbital density matrices, molecular coordinates, and basis functions of these molecules were obtained from the magnetic shielding calculation at the same level of theory in the NICS calculation (*vide supra*). The GIMIC calculations were performed using the GIMIC program (ver. 2.1.4). The input files for the GIMIC program were generated using the Gaussian2gimic.py script.[28] Each current strength was calculated by numerical integration of the current density flowing across a plane perpendicularly to the molecular plane and bisecting the chosen chemical bond. The current paths are represented by red or blue arrows in Figure S5. The clockwise and counterclockwise current flows correspond to diatropic (red) and paratropic (blue) ring currents, respectively. The current strength is given in nA/T. The signed modulus of the current densities (Figure S6) is visualized using the ParaView program (version 5.8.1).[29] The grid information for the calculations of the current density was obtained using the Multiwfn program.[30]

There are diatropic current flows in all benzene and thiophene rings. On the other hand, the paratropic currents flow in all four-membered rings. The results of the GIMIC calculations are well in line with the NICS analyses.

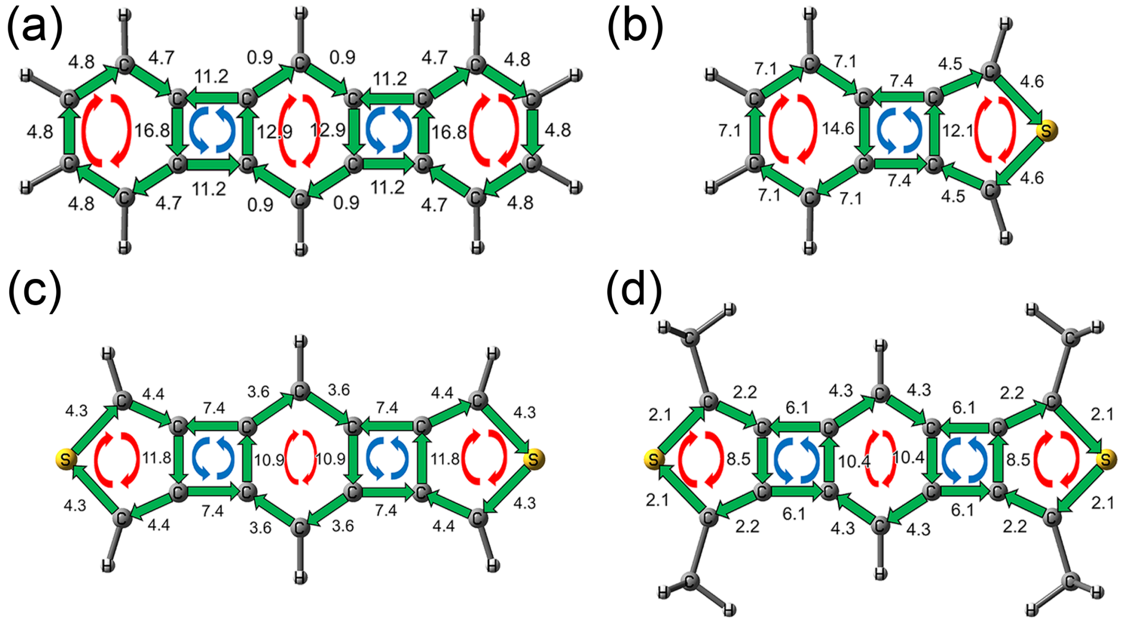

Figure S5. The calculated current paths and strengths (nA/T) for [3]phenylene (a), ***c*BCT** (b), **BBCT** (c), and **BBCT-Me** (d).

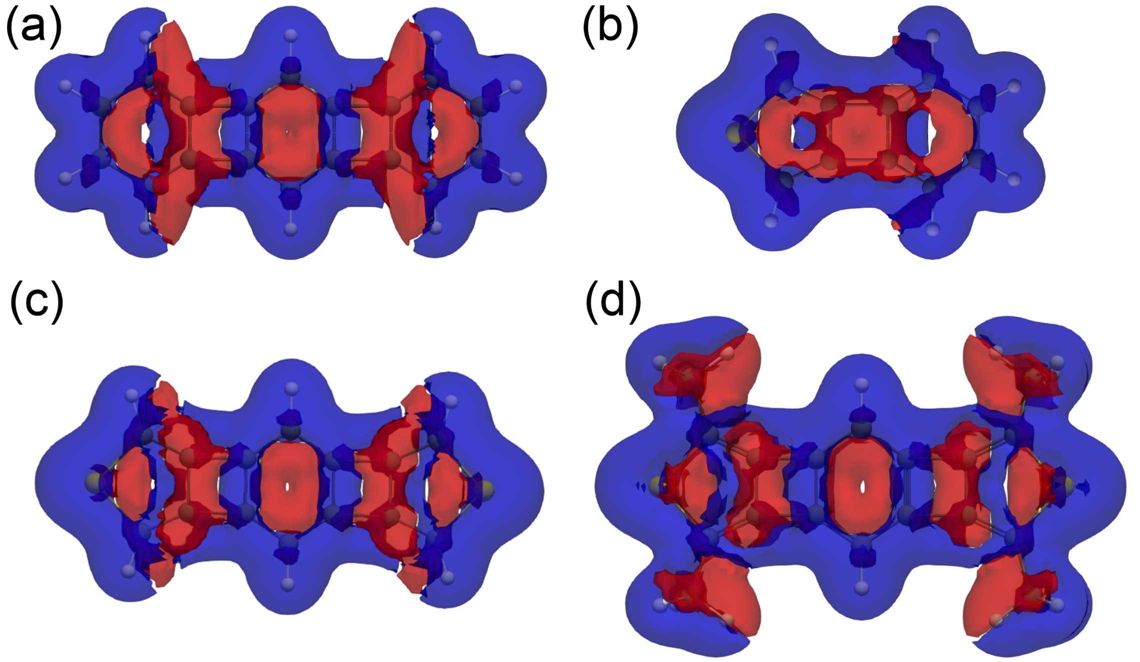

Figure S6. The calculated signed modulus of the current densities (isovalue: 0.01 a.u.; red and blue regions are indicate paratropic and diatropic current densities, respectively) for [3]phenylene (a), ***c*BCT** (b), **BBCT** (c), and **BBCT-Me** (d).

5. Details of X-Ray Single Crystal Analysis, and HOMA, NCI, and Charge Transfer Integrals Calculations

Single crystals of **BBCT** and **BBCT-Me** suitable for X-ray diffraction study were grown from EtOH/THF and hexane/CH_2Cl_2, respectively, that are subjected to data collection. X-ray crystallography was performed on a Rigaku Mercury charge-coupled device (CCD) diffractometer at 173 K with graphite monochromated Mo-$K\alpha$ radiation (γ = 0.71073 Å) up to $2\theta_{\max}$ = 60.6°. All calculations were performed using the CrystalStructure crystallographic software package,[31] and structural refinements were done using the SHELXL Version 2014/7 program.[32] Visualization of the molecular packing structures was performed by the Mercury software.[33] The crystallographic data are summarized in Tables S6 and S7. The crystallographic data have been deposited to the Cambridge Crystallographic Data Center: Deposition numbers 2223524 for **BBCT** and 2223525 for **BBCT-Me**. Copies of the data can be obtained free of charge via http://www.ccdc.cam.ac.uk/conts/retrieving.html (or from Cambridge Crystallographic Data Centre, 12, Union Road, Cambridge, CB2 1EZ, UK; Fax+44 1223 336033; e-mail: deposit@ccdc.cam.ac.uk).

The atom numberings and bond lengths of **BBCT** and **BBCT-Me** are shown in Figures S7 and S8.

5–1. Crystal Structure of BBCT

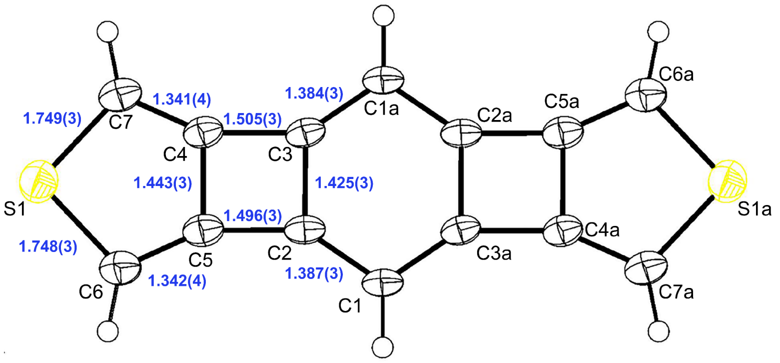

Figure S7. ORTEP diagram (50% probability level) of **BBCT**.

Table S6. Crystal data and structure analysis results for **BBCT**.

Identification code	**BBCT**	Density	1.540 g/cm^3
Empirical formula	$C_{14}H_6S_2$	Absorption coefficient	4.780 cm^{-1}
Formula weight	238.32	F(000)	244
Temperature	173 K	Crystal size	0.300 × 0.200 × 0.010 mm^3
Wavelength	0.71073 Å	Reflections collected	6153
Crystal system	monoclinic	Independent reflections	1408 (R_{int} = 0.0484)
Space group	$P2_1/c$	Absorption correction	empirical
Unit cell dimensions	a = 12.2173(14) Å	Refinement method	Full-matrix least-squares on F^2
	b = 7.2881(8) Å	Data / restraints / parameters	1408 / 0 / 73
	c = 5.7720(6) Å	Goodness of fit	1.08
	β = 90.868(10)°	Final R indices [I>2sigma(I)]	R_1 = 0.0552, wR_2 = 0.1123
Volume	V = 513.89(10) Å^3	R indices (all data)	R = 0.1008, wR_2 = 0.1123
Z	2	Largest diff. peak and hole	0.34 and –0.24 e/Å^3

5–2. Crystal Structure of BBCT-Me.

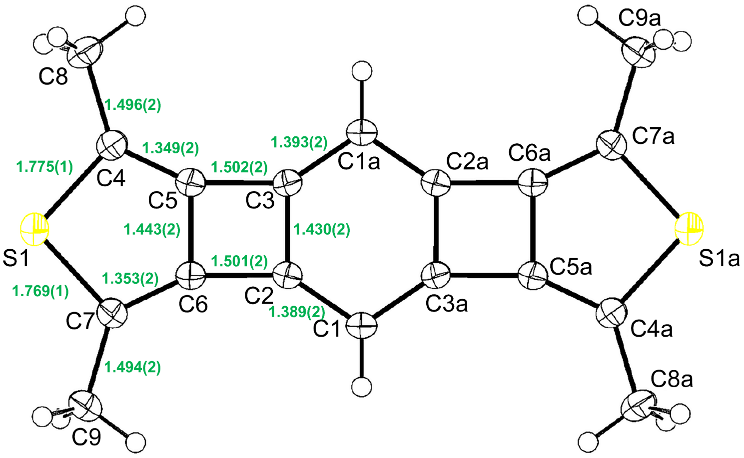

Figure S8. ORTEP diagram (50% probability level) of **BBCT-Me**.

Table S7. Crystal data and structure analysis results for **BBCT-Me**.

Identification code	**BBCT-Me**	Density	1.346 g/cm^3
Empirical formula	$C_{18}H_{14}S_2$	Absorption coefficient	3.521 cm^{-1}
Formula weight	294.43	F(000)	308
Temperature	173 K	Crystal size	0.100 × 0.100 × 0.100 mm^3
Wavelength	0.71073 Å	Reflections collected	8877
Crystal system	monoclinic	Independent reflections	1965 (R_{int} = 0.0143)
Space group	$P2_1/c$	Absorption correction	empirical
Unit cell dimensions	a = 5.9039(2) Å	Refinement method	Full-matrix least-squares on F^2
	b = 16.2762(6) Å	Data / restraints / parameters	1965 / 0 / 93
	c = 7.6534(3) Å	Goodness of fit	1.09
	β = 98.902(4)°	Final R indices [I>2sigma(I)]	R_1 = 0.0311, wR_2 = 0.0972
Volume	V = 726.58(5) Å^3	R indices (all data)	R = 0.0343, wR_2 = 0.0972
Z	2	Largest diff. peak and hole	0.35 and –0.30 e/Å^3

5–3. HOMA Analysis

We employed HOMA as the structural criterion for local aromaticity and non-aromaticity of the benzene and thiophene rings of **BBCT**s using their crystal structures.[34] The HOMA values of the benzene rings were calculated using eq 1 with individual bond lengths, R_i:

$$\mathrm{HOMA} = 1 - \frac{\alpha_{CC}}{6}\sum_{i}^{6}\left(R_{\mathrm{opt,CC}} - R_{\mathrm{CC},i}\right)^2 \tag{1}$$

and the HOMA values of the thiophene rings were calculated using eq 2:

$$\mathrm{HOMA} = 1 - \left\{\frac{\alpha_{\mathrm{CC}}}{3}\sum_{i}^{3}\left(R_{\mathrm{opt,CC}} - R_{\mathrm{CC},i}\right)^2 + \frac{\alpha_{\mathrm{CS}}}{2}\sum_{i}^{2}\left(R_{\mathrm{opt,CS}} - R_{\mathrm{CS},i}\right)^2\right\} \tag{2}$$

where the subscripts CC and CS denote carbon–carbon and carbon–sulfur bonds, respectively. The optimal bond lengths R_{opt} and constants α were derived from eq 3 and 4, respectively:

$$R_{\mathrm{opt,j}} = \left(\mathrm{R}_{\mathrm{s,j}} + wR_{\mathrm{d,j}}\right)/(1 + w) \tag{3}$$

$$\alpha_{\mathrm{j}} = 2\left[\left(R_{s,j} - R_{\mathrm{opt,j}}\right)^2 + \left(R_{\mathrm{d,j}} - R_{\mathrm{opt,j}}\right)^2\right]^{-1} \tag{4}$$

In these equations, the subscript j denotes the bond type (CC or CS, not single or double bond); R_{s} and R_{d} correspond to the reference lengths for single and double bonds, respectively; and w is the ratio of force constants for double and single bonds. The values of R_{opt} and α were obtained from the literature.[35] HOMA values close to 1 indicate a high degree of cyclic π-electron delocalization, and smaller values indicate poor π-electron delocalization.

The HOMA values of the benzene rings of the **BBCT**s are 0.88 and 0.85 (Figure S9). On the other hand, the HOMA values of the thiophene rings of the **BBCT**s are negative, showing small degree of π-electron delocalization.

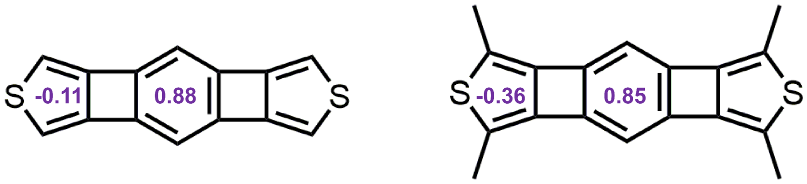

Figure S9. HOMA values at the benzene and thiophene rings of **BBCT** and **BBCT-Me**.

5–4. Noncovalent Interaction (NCI) Plots

We performed a noncovalent interaction (NCI) analysis in order to investigate intermolecular interactions in the crystal packing structures (Figures 4d–f, 5d–f, S10, and S11).[36] This analysis visualizes the regions showing van der Waals interactions as green-colored isosurfaces, and the regions showing attractive or repulsive forces as blue- or red-colored isosurfaces, respectively. The wavefunctions required for these analyses were calculated using the composite method r^2SCAN-3c,[37] which is the recently developed DFT functional underlying the r^2SCAN functional[38] by Stefan Grimme and co-workers for the fast and accurate estimation of noncovalent interactions. This DFT functional is one of the most recommended methods as mentioned in a recent review article.[39] This DFT functional includes the atom-pairwise dispersion correction based on tight binding partial charges (D4),[40,41] and the empirical geometrical counterpoise (gCP) scheme[42] for the correction of intra- and intermolecular basis set super position errors (BSSE).[43] We used the def2-mTZVPP basis set,[37] which is a modified version of the def2-TZVP.[44,45] To reduce the computational effort, the resolution-of-identity (RI) approximation for Coulomb integrals (RI-J) was applied,[46] and the corresponding auxiliary Coulomb fitting basis (def2-mTZVPP/J) was utilized. The calculations of r^2SCAN-3c were performed by the ORCA 5.0.2[47–49] program combined with the SHARK module[50] using "TightSCF" convergence criteria for each SCF calculation. The calculations for the NCI analysis were carried out using the Multiwfn program (ver. 3.8).[30] The visualization of NCI isosurfaces was performed using the VMD program (ver. 1.9.3).[51] The 2D reduced density gradient vs. sign(λ_2)ρ plots (Figures S10 and S11) were visualized using the Gnuplot 5.4 program.[52]

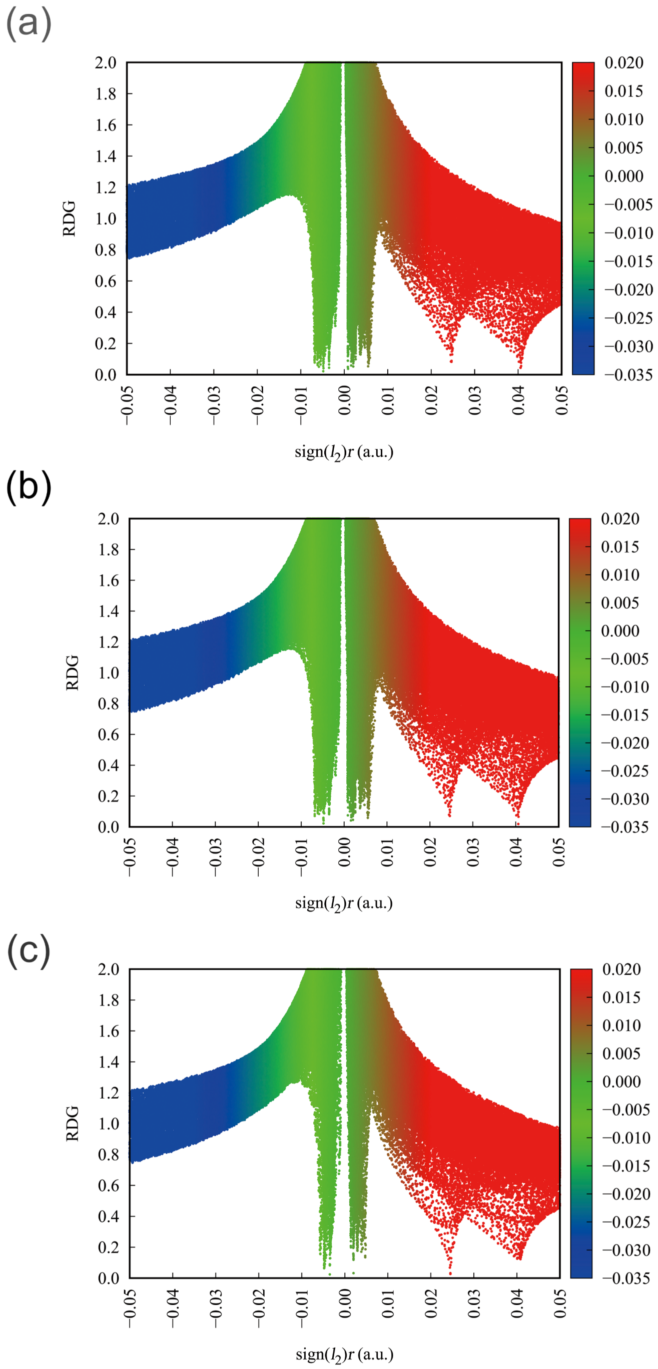

Figure S10. (a–c) 2D reduced density gradient vs. sign(λ_2)ρ plots corresponding to the NCI plots of the crystal packing structure of **BBCT** in Figs. 4d (a), 4e (b), and 4f (c).

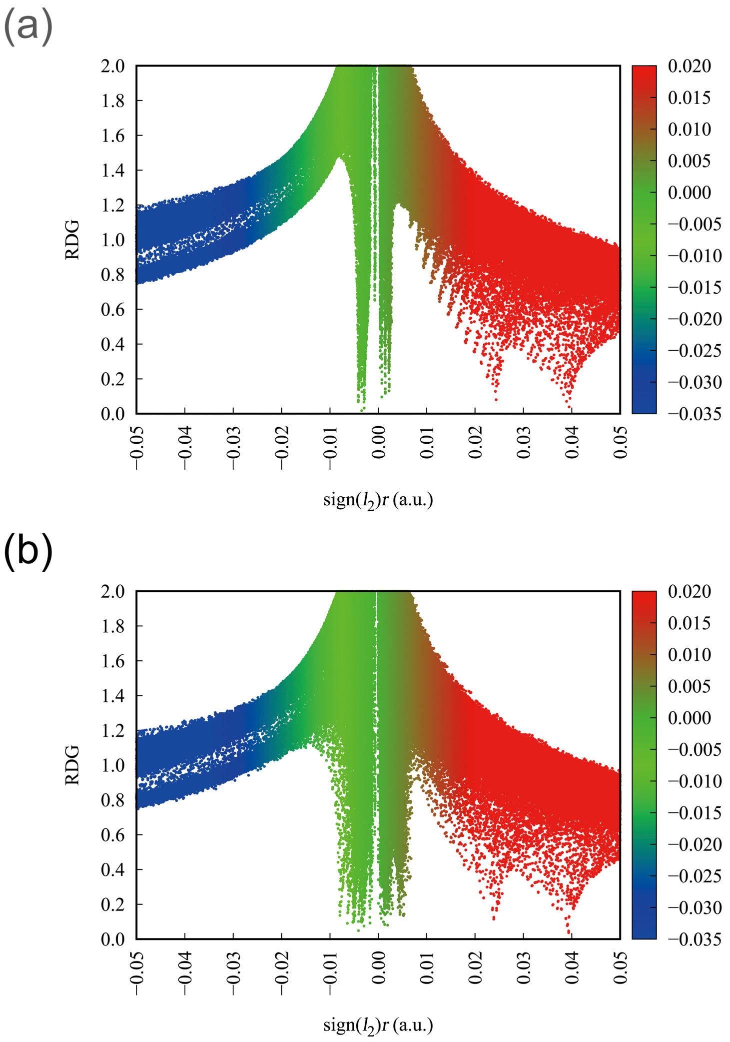

Figure S11. (a) 2D reduced density gradient vs. sign(λ_2)ρ plots corresponding to the NCI plots of the crystal packing structure of **BBCT-Me** in Figs. 5d and f. (b) 2D reduced density gradient vs. sign(λ_2)ρ plot corresponding to the NCI plot of the crystal packing structure of **BBCT-Me** in Fig. 5e.

5–5. Charge Transfer Integrals Calculations

We calculated the effective transfer integrals (t) between the HOMOs in the dimers extracted from the crystal structure of **BBCT** using the Amsterdam Density Functional (ADF) program package[53–55] at GGA-type functional PW91[56]/TZP[57] level of theory. Calculated transfer integrals (t_a and t_p) are shown in Figure S12.

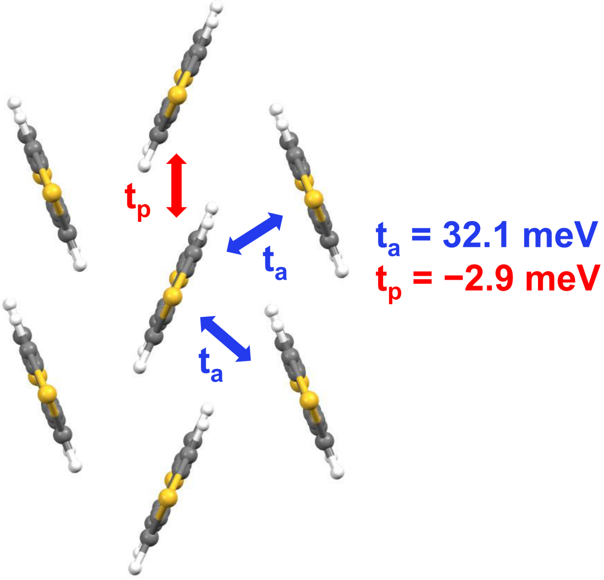

Figure S12. Calculated transfer integrals of the two different dimers in the herringbone structure of **BBCT**.

6. ^{1}H and/or ^{13}C{^{1}H} NMR Spectra of All Compounds

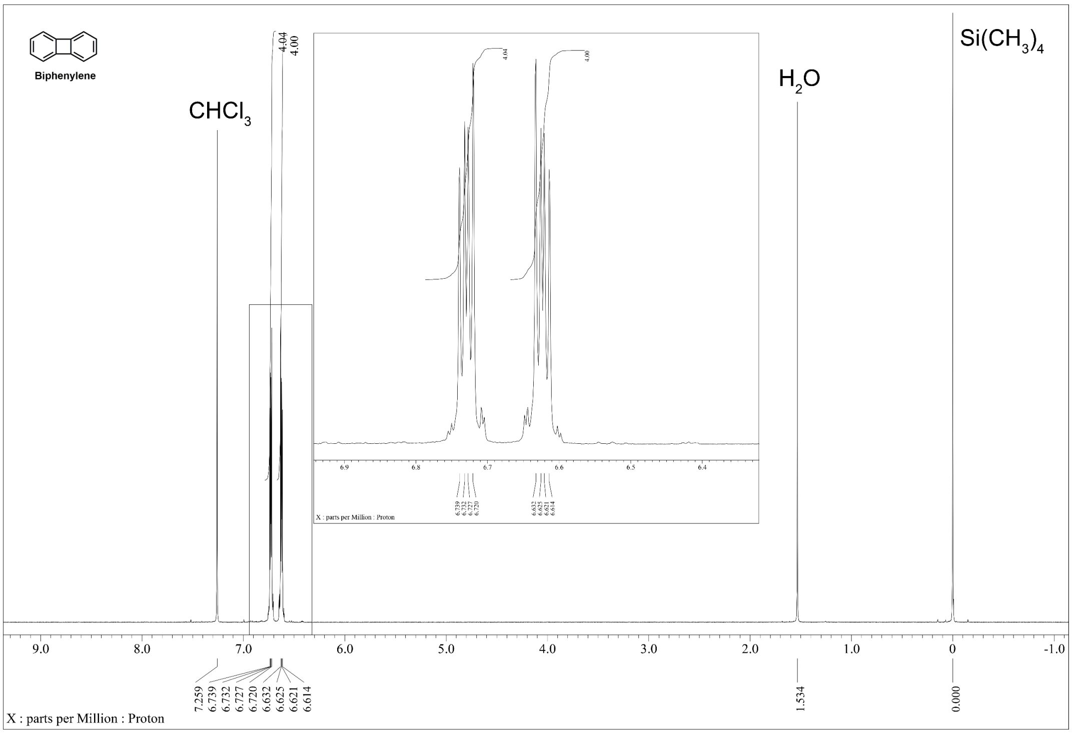

Figure S13. ^{1}H (500 MHz) NMR spectrum of biphenylene in $CDCl_3$ at 25 °C.

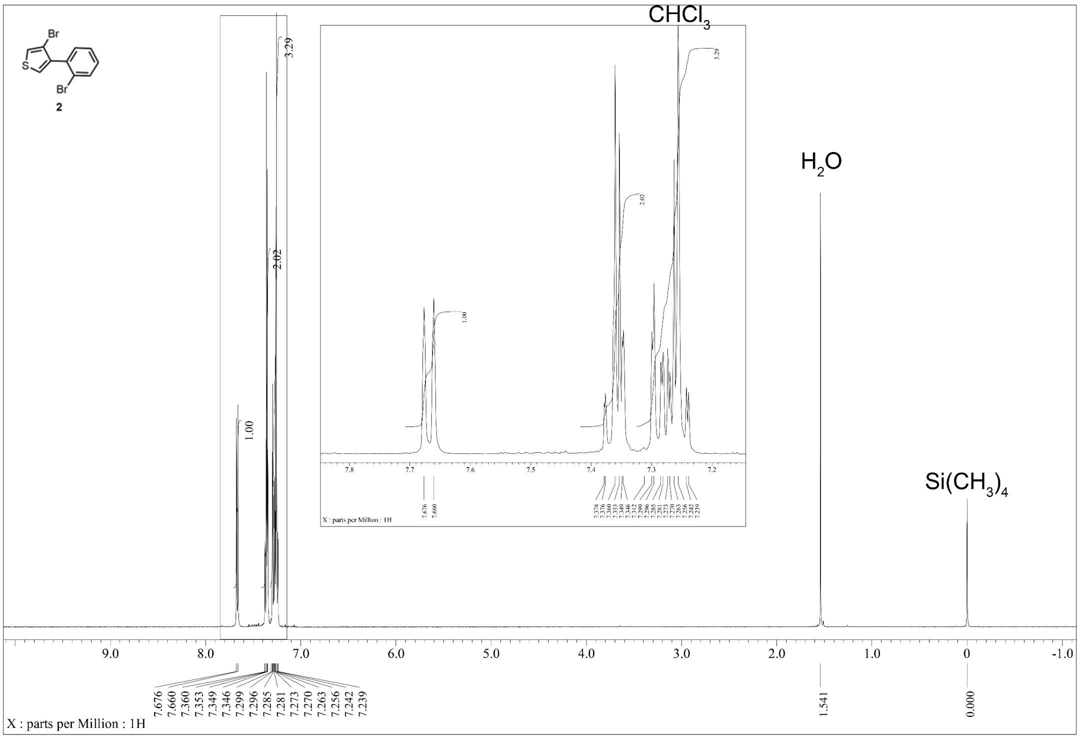

Figure S14. ^{1}H (500 MHz) NMR spectrum of **2** in $CDCl_3$ at 26 °C.

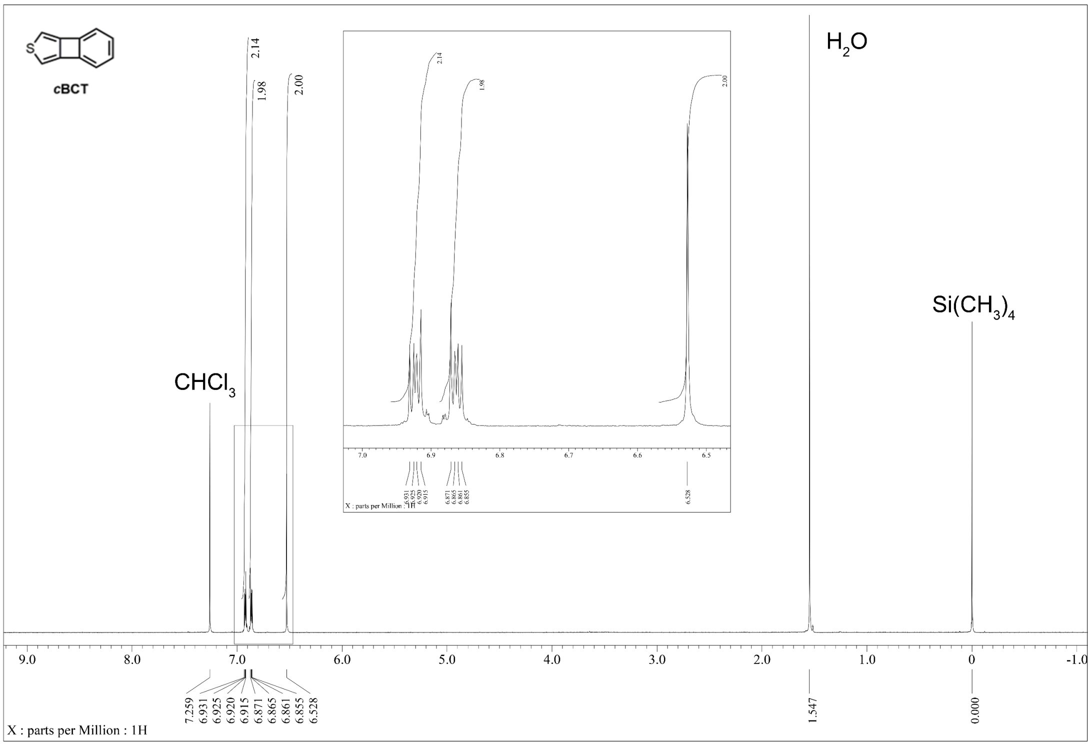

Figure S15. ^{1}H (500 MHz) NMR spectrum of ***c*BCT** in $CDCl_3$ at 26 °C.

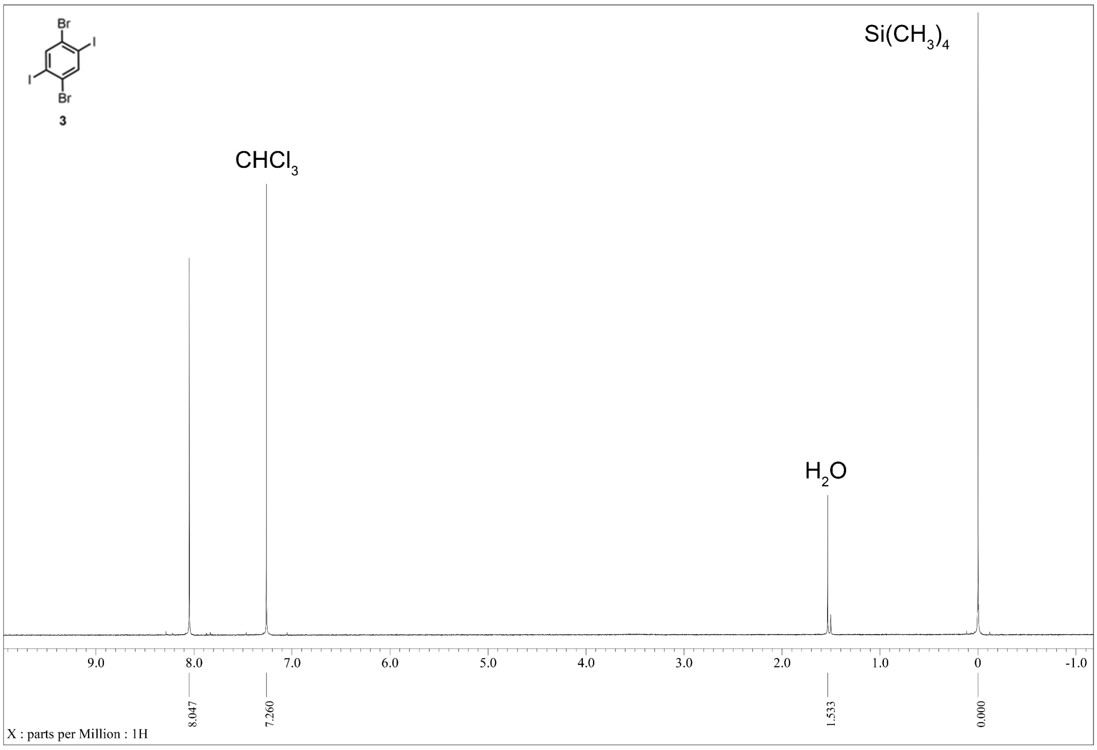

Figure S16. ^{1}H (500 MHz) NMR spectrum of **3** in $CDCl_3$ at 25 °C.

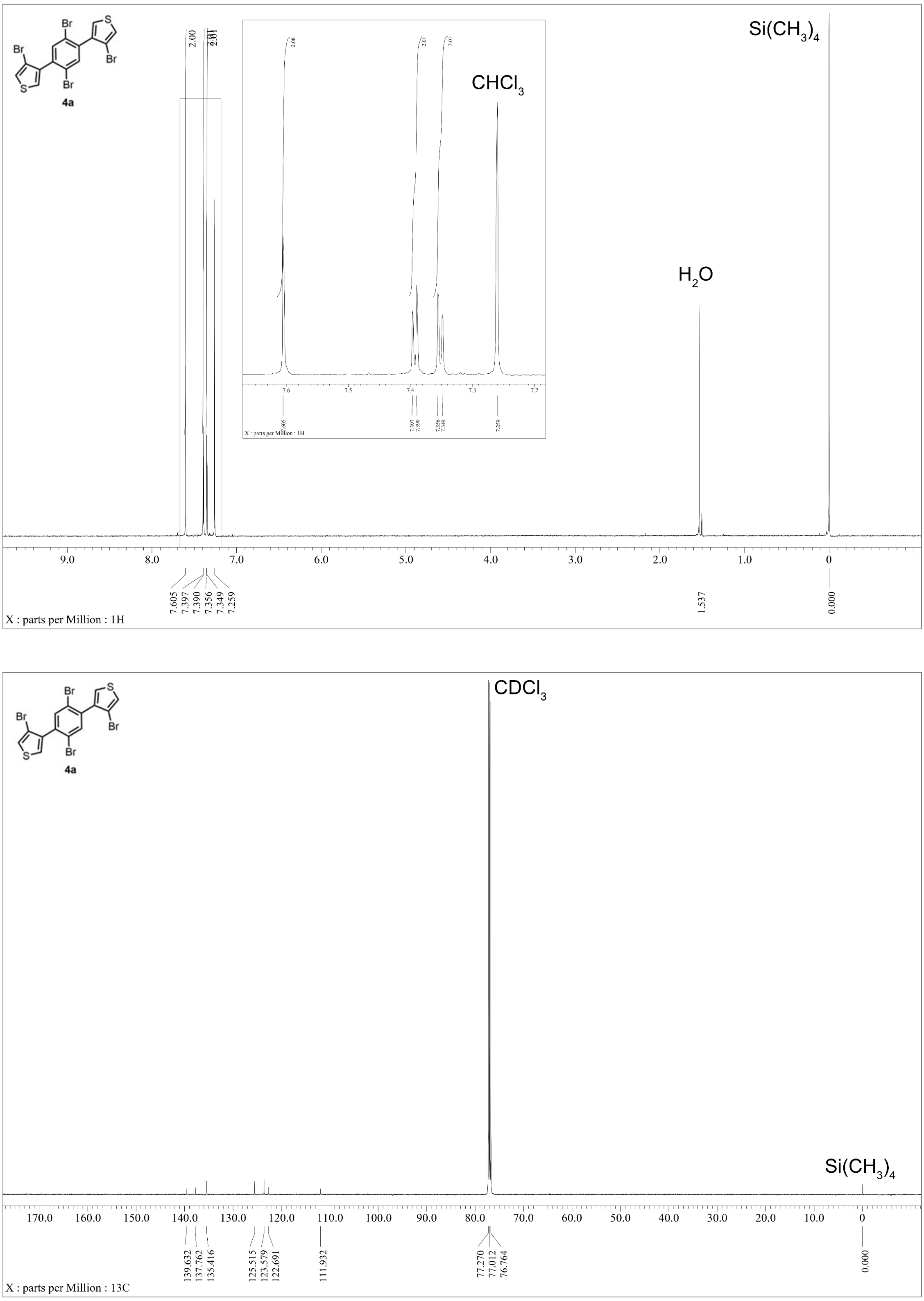

Figure S17. ^{1}H (top, 500 MHz) and ^{13}C{^{1}H} (bottom, 126 MHz) NMR spectra of **4a** in CDCl$_3$ at 25 °C.

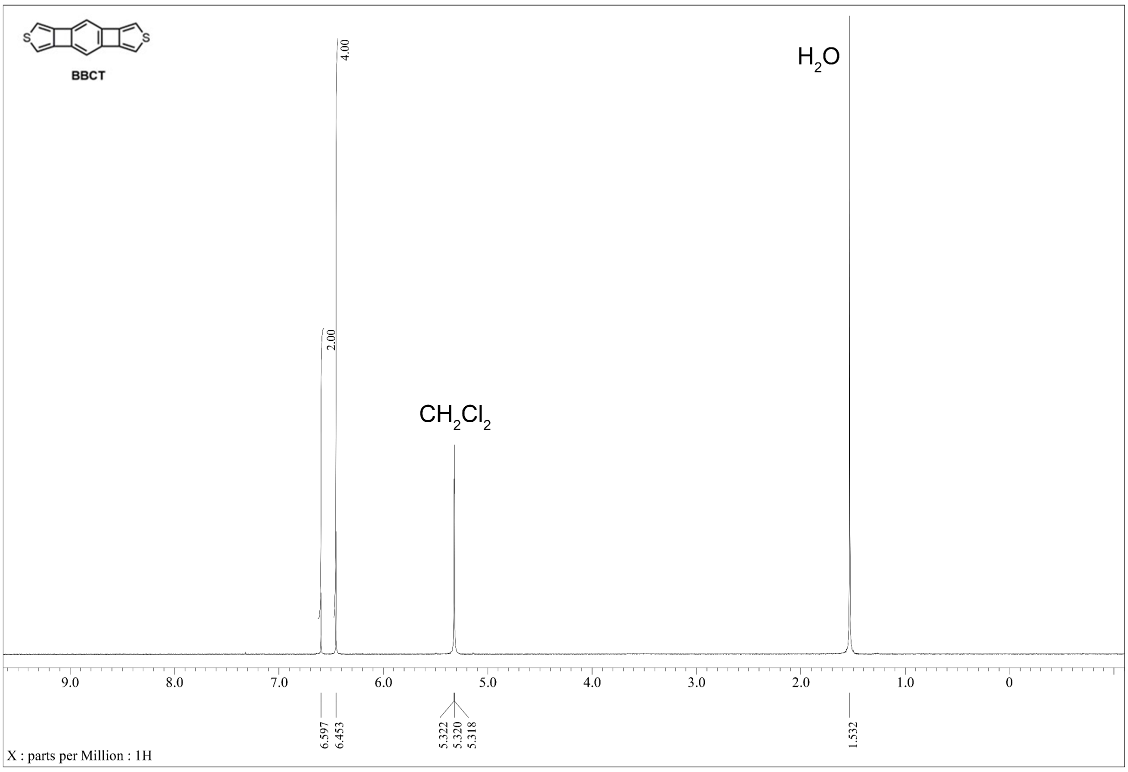

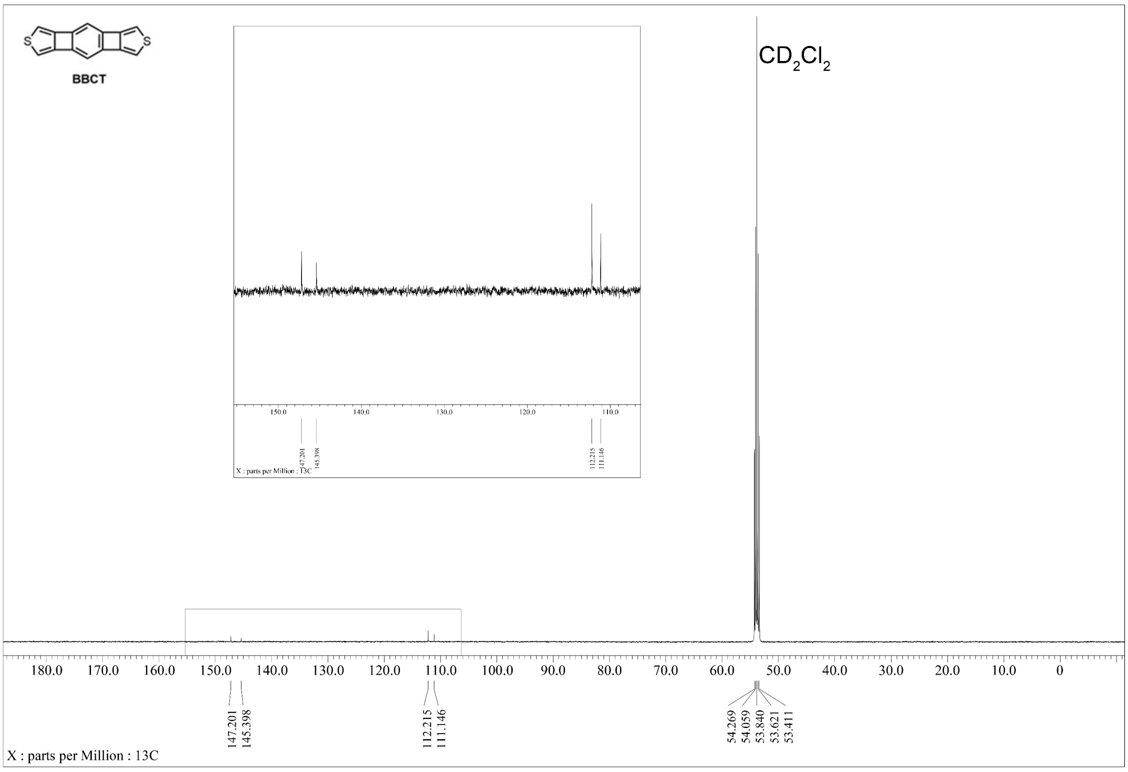

Figure S18. ^{1}H (top, 500 MHz) and ^{13}C{^{1}H} (bottom, 126 MHz) NMR spectra of **BBCT** in CD_2Cl_2. at 25 °C.

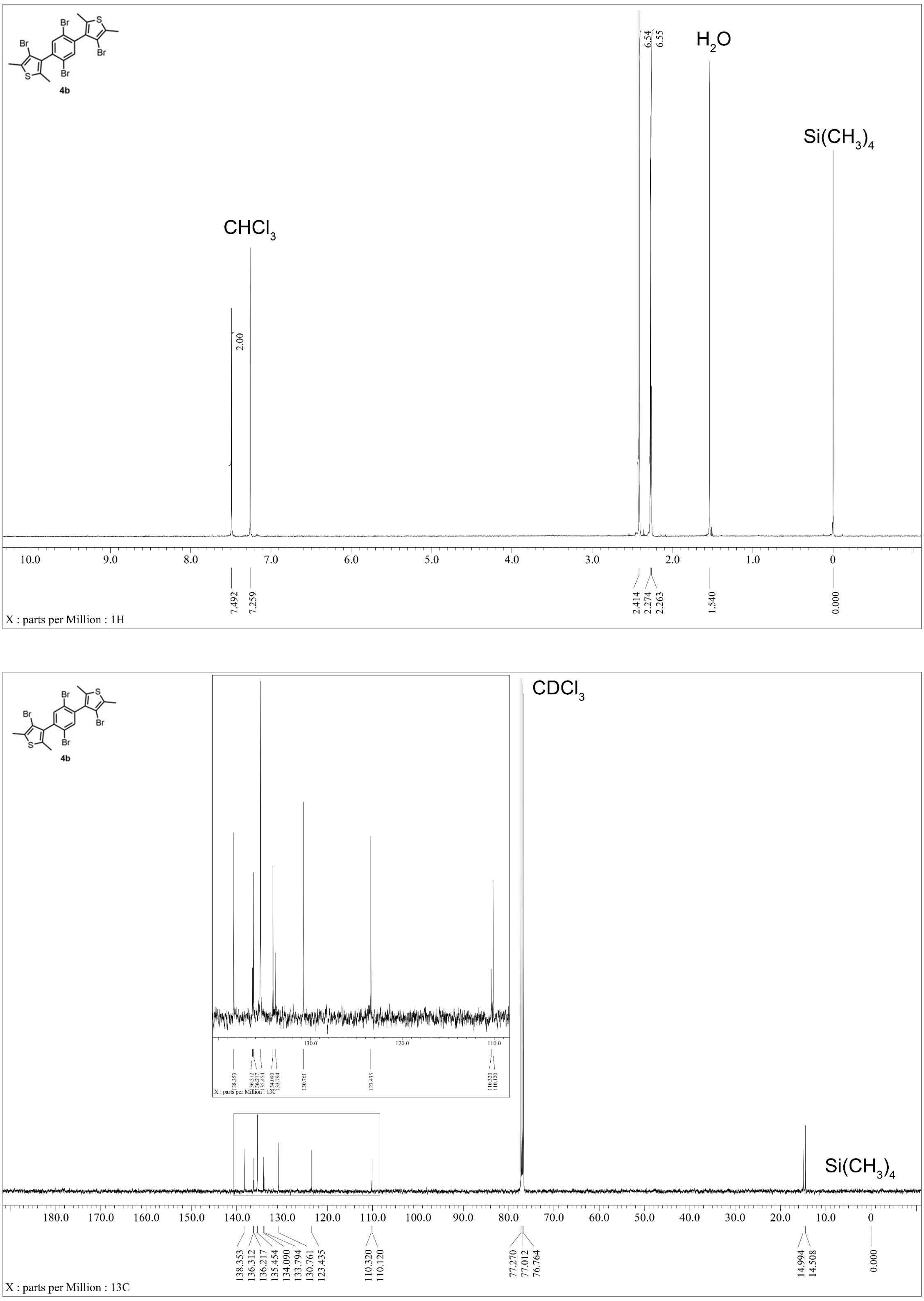

Figure S19. ^{1}H (top, 500 MHz) and ^{13}C{^{1}H} (bottom, 126 MHz) NMR spectra of **4b** in CDCl$_3$ at 25 °C.

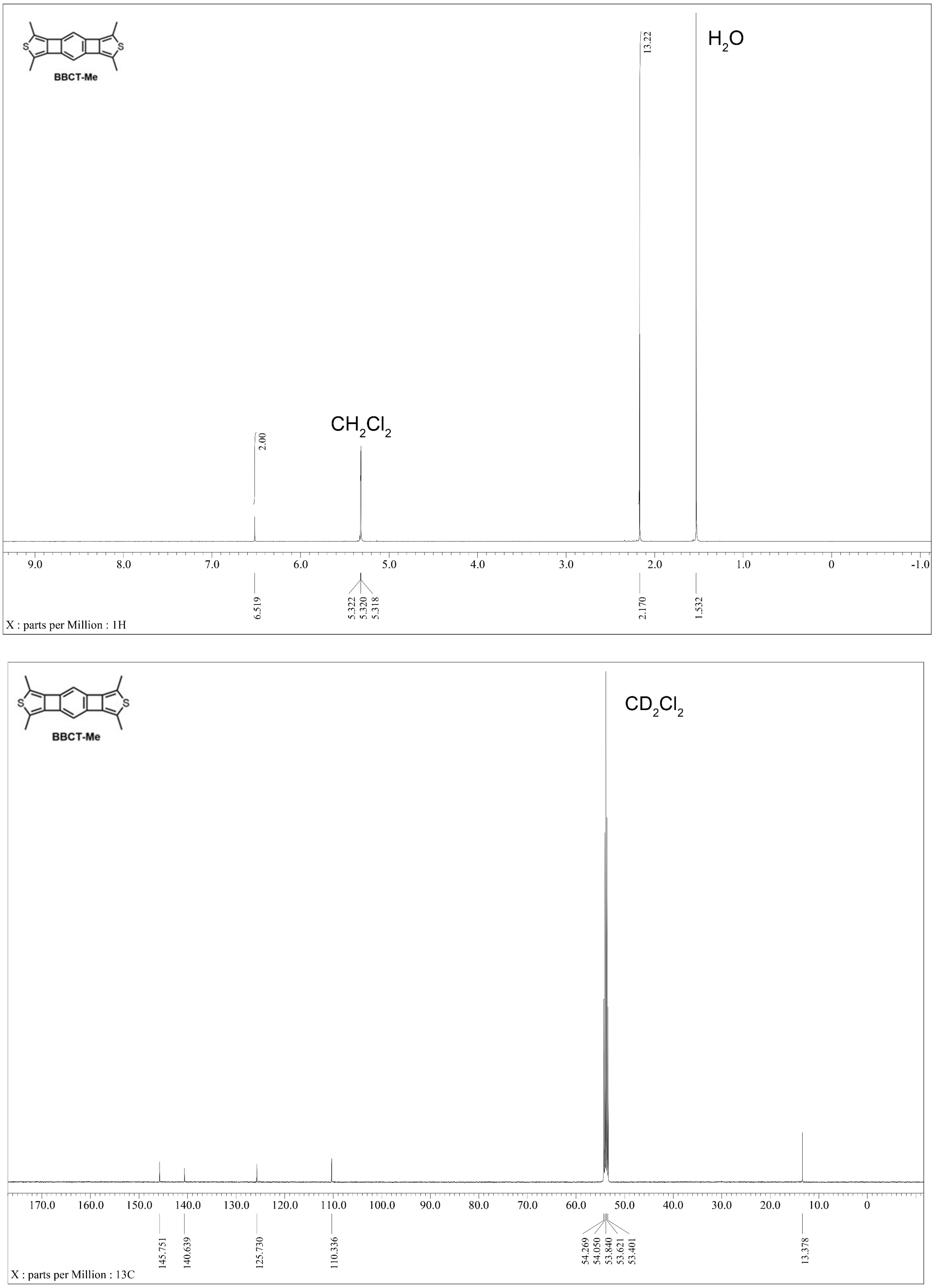

Figure S20. ^{1}H (top, 500 MHz) and ^{13}C{^{1}H} (bottom, 126 MHz) NMR spectra of **BBCT-Me** in CD_2Cl_2 at 25 °C.

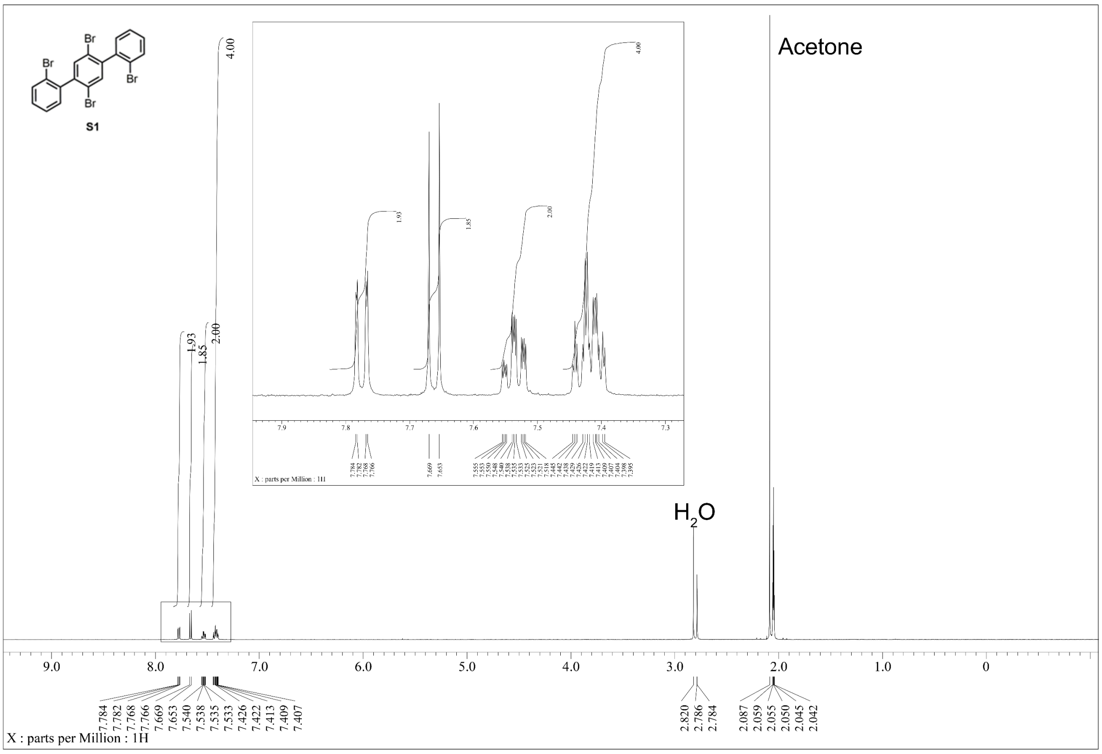

Figure S21. ^{1}H (500 MHz) NMR spectrum of **S1** in acetone-d_6 at 25 °C.

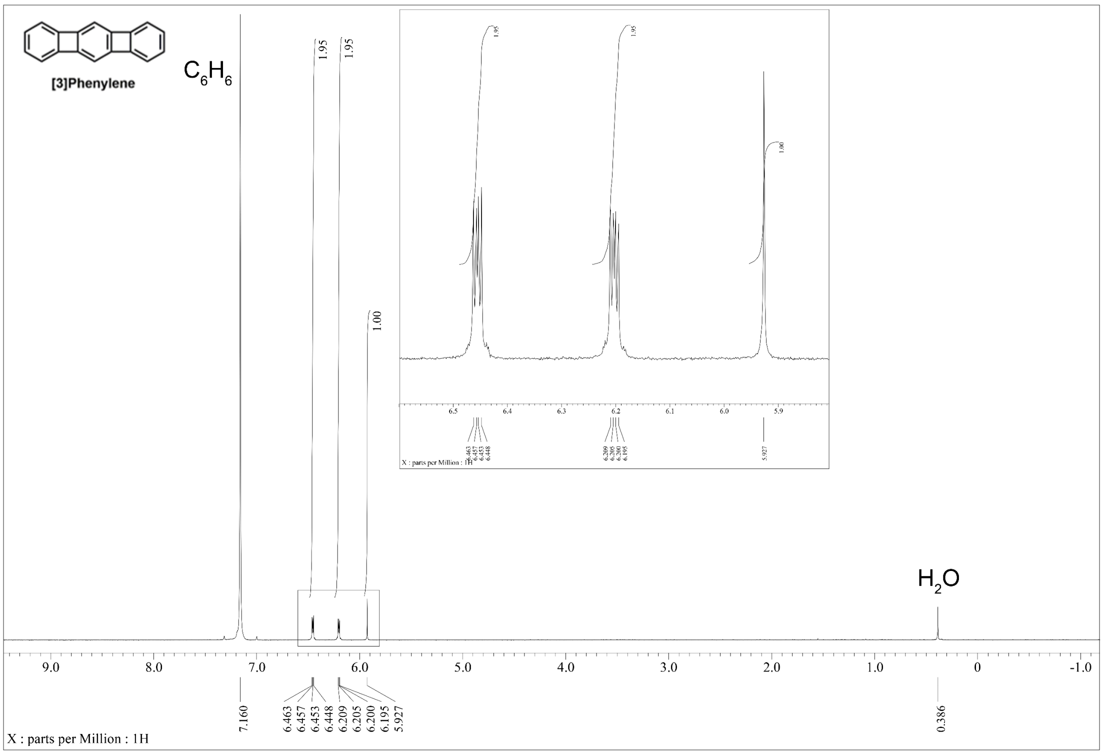

Figure S22. ^{1}H (500 MHz) NMR spectrum of [3]phenylene in C$_6$D$_6$ at 25 °C.

7. Cartesian Coordinates of All Optimized Geometries

BBCT

Symbol	X	Y	Z
C	0.000000	0.000000	1.490395
C	0.000000	1.154322	0.712379
C	0.000000	1.154322	-0.712379
C	0.000000	0.000000	-1.490395
C	0.000000	-1.154322	-0.712379
C	0.000000	-1.154322	0.712379
H	0.000000	0.000000	2.573056
H	0.000000	0.000000	-2.573056
C	0.000000	2.653817	-0.722490
C	0.000000	3.880351	-1.283165
C	0.000000	2.653817	0.722490
S	0.000000	5.103606	0.000000
H	0.000000	4.200319	-2.313876
C	0.000000	3.880351	1.283165
H	0.000000	4.200319	2.313876
C	0.000000	-2.653817	-0.722490
C	0.000000	-3.880351	-1.283165
C	0.000000	-2.653817	0.722490
S	0.000000	-5.103606	0.000000
H	0.000000	-4.200319	-2.313876
C	0.000000	-3.880351	1.283165
H	0.000000	-4.200319	2.313876

Zero-point correction= 0.147901 (Hartree/Particle)
Thermal Correction to Energy= 0.159492
Thermal Correction to Enthalpy= 0.160437
Thermal Correction to Gibbs Free Energy= 0.110726
Sum of electronic and zero-point energies= -1333.338789
Sum of electronic and thermal Energies = -1333.327198
Sum of electronic and thermal Enthalpy = -1333.326254
Sum of electronic and thermal Free Energy Correction= -1333.375964

BBCT-Me (S_0)

Symbol	X	Y	Z
C	-3.870197	1.308594	0.000000
C	-2.655029	0.723712	0.000000
C	-2.655029	-0.723712	0.000000
C	-3.870197	-1.308594	0.000000
S	-5.097011	0.000000	0.000000
C	3.870197	-1.308594	0.000000
C	2.655029	-0.723712	0.000000
C	2.655029	0.723712	0.000000
C	3.870197	1.308594	0.000000
S	5.097011	0.000000	0.000000
C	1.157094	0.713396	0.000000
C	0.000000	1.488605	0.000000
C	-1.157094	0.713396	0.000000
C	-1.157094	-0.713396	0.000000
C	0.000000	-1.488605	0.000000
C	1.157094	-0.713396	0.000000
H	0.000000	2.571616	0.000000
H	0.000000	-2.571616	0.000000
C	4.290245	2.743515	0.000000
H	3.408654	3.387602	0.000000
H	4.888858	2.989751	0.882591
C	4.290245	-2.743515	0.000000
H	3.408654	-3.387602	0.000000
H	4.888858	-2.989751	-0.882591
C	-4.290245	2.743515	0.000000
H	-3.408654	3.387602	0.000000
H	-4.888858	2.989751	-0.882591
C	-4.290245	-2.743515	0.000000
H	-4.888858	-2.989751	-0.882591
H	-3.408654	-3.387602	0.000000
H	-4.888858	-2.989751	0.882591
H	-4.888858	2.989751	0.882591
H	4.888858	2.989751	-0.882591
H	4.888858	-2.989751	0.882591

Zero-point correction= 0.258059 (Hartree/Particle)

Thermal Correction to Energy= 0.27718

Thermal Correction to Enthalpy= 0.278124

Thermal Correction to Gibbs Free Energy= 0.211682

Sum of electronic and zero-point energies= -1490.547856

Sum of electronic and thermal Energies = -1490.528735

Sum of electronic and thermal Enthalpy = -1490.527791

Sum of electronic and thermal Free Energy Correction= -1490.594233

BBCT-Me (S_1)

Symbol	X	Y	Z
C	-3.845577	1.312406	0.000000
C	-2.602493	0.735620	0.000000
C	-2.602493	-0.735620	0.000000
C	-3.845577	-1.312406	0.000000
S	-5.027717	0.000000	0.000000
C	3.845577	-1.312406	0.000000
C	2.602493	-0.735620	0.000000
C	2.602493	0.735620	0.000000
C	3.845577	1.312406	0.000000
S	5.027717	0.000000	0.000000
C	1.155151	0.752936	0.000000
C	0.000000	1.524674	0.000000
C	-1.155151	0.752936	0.000000
C	-1.155151	-0.752936	0.000000
C	0.000000	-1.524674	0.000000
C	1.155151	-0.752936	0.000000
H	0.000000	2.608996	0.000000
H	0.000000	-2.608996	0.000000
C	4.275361	2.745227	0.000000
H	3.392698	3.387705	0.000000
H	4.871328	2.997775	0.883309
C	4.275361	-2.745227	0.000000
H	3.392698	-3.387705	0.000000

H	4.871328	-2.997775	-0.883309
C	-4.275361	2.745227	0.000000
H	-3.392698	3.387705	0.000000
H	-4.871328	2.997775	-0.883309
C	-4.275361	-2.745227	0.000000
H	-4.871328	-2.997775	-0.883309
H	-3.392698	-3.387705	0.000000
H	-4.871328	-2.997775	0.883309
H	-4.871328	2.997775	0.883309
H	4.871328	2.997775	-0.883309
H	4.871328	-2.997775	0.883309

***c*BCT**

Symbol	X	Y	Z
C	0.000000	1.444872	-2.001815
C	0.000000	0.711543	-0.838958
C	0.000000	-0.711543	-0.838958
C	0.000000	-1.444872	-2.001815
C	0.000000	-0.696068	-3.201207
C	0.000000	0.696068	-3.201207
H	0.000000	2.528167	-2.021043
H	0.000000	-2.528167	-2.021043
H	0.000000	-1.220982	-4.149905
H	0.000000	1.220982	-4.149905
C	0.000000	-0.722597	0.663339
C	0.000000	-1.282667	1.890974
C	0.000000	0.722597	0.663339
S	0.000000	0.000000	3.110605
H	0.000000	-2.313035	2.212112
C	0.000000	1.282667	1.890974
H	0.000000	2.313035	2.212112

Zero-point correction= 0.124212 (Hartree/Particle)
Thermal Correction to Energy= 0.132066
Thermal Correction to Enthalpy= 0.133010

Thermal Correction to Gibbs Free Energy= 0.091780

Sum of electronic and zero-point energies= -782.773330

Sum of electronic and thermal Energies = -782.765476

Sum of electronic and thermal Enthalpy = -782.764532

Sum of electronic and thermal Free Energy Correction= -782.805762

[3]Phenylene

Symbol	X	Y	Z
C	0.000000	5.030416	0.692728
C	0.000000	3.821782	1.443515
C	0.000000	2.664674	0.711276
C	0.000000	2.664674	-0.711276
C	0.000000	3.821782	-1.443515
C	0.000000	5.030416	-0.692728
H	0.000000	5.977411	1.220733
H	0.000000	3.842180	2.526992
H	0.000000	3.842180	-2.526992
H	0.000000	5.977411	-1.220733
C	0.000000	1.155743	0.709051
C	0.000000	0.000000	1.485741
C	0.000000	1.155743	-0.709051
C	0.000000	-1.155743	0.709051
H	0.000000	0.000000	2.568879
C	0.000000	0.000000	-1.485741
C	0.000000	-1.155743	-0.709051
H	0.000000	0.000000	-2.568879
C	0.000000	-2.664674	-0.711276
C	0.000000	-2.664674	0.711276
C	0.000000	-3.821782	-1.443515
C	0.000000	-3.821782	1.443515
C	0.000000	-5.030416	-0.692728
H	0.000000	-3.842180	-2.526992
C	0.000000	-5.030416	0.692728
H	0.000000	-3.842180	2.526992
H	0.000000	-5.977411	-1.220733

H	0.000000	-5.977411	1.220733

Zero-point correction= 0.214516 (Hartree/Particle)

Thermal Correction to Energy= 0.226708

Thermal Correction to Enthalpy= 0.227652

Thermal Correction to Gibbs Free Energy= 0.177058

Sum of electronic and zero-point energies= -691.760004

Sum of electronic and thermal Energies = -691.747812

Sum of electronic and thermal Enthalpy = -691.746868

Sum of electronic and thermal Free Energy Correction= -691.797462

Biphenylene

Symbol	X	Y	Z
C	0.0000000	0.6941110	3.1190490
C	0.0000000	1.4430590	1.9141640
C	0.0000000	0.7110400	0.7544280
C	0.0000000	-0.7110400	0.7544280
C	0.0000000	-1.4430590	1.9141640
C	0.0000000	-0.6941110	3.1190490
H	0.0000000	1.2209370	4.0667720
H	0.0000000	2.5266560	1.9344140
H	0.0000000	-2.5266560	1.9344140
H	0.0000000	-1.2209370	4.0667720
C	0.0000000	0.7110400	-0.7544280
C	0.0000000	1.4430590	-1.9141640
C	0.0000000	-0.7110400	-0.7544280
C	0.0000000	0.6941110	-3.1190490
H	0.0000000	2.5266560	-1.9344140
C	0.0000000	-1.4430590	-1.9141640
C	0.0000000	-0.6941110	-3.1190490
H	0.0000000	1.2209370	-4.0667720
H	0.0000000	-2.5266560	-1.9344140
H	0.0000000	-1.2209370	-4.0667720

Zero-point correction= 0.157576 (Hartree/Particle)

Thermal Correction to Energy= 0.165723

Thermal Correction to Enthalpy= 0.166668

Thermal Correction to Gibbs Free Energy= 0.125660

Sum of electronic and zero-point energies= -461.984806

Sum of electronic and thermal Energies = -461.976659

Sum of electronic and thermal Enthalpy = -461.975715

Sum of electronic and thermal Free Energy Correction= -462.016723

8. References

1. D. R. Coulson, L. C. Satek and S. O. Grim, Tetrakis-(triphenylphosphine)palladium. *Inorg. Synth.,* 1972, **13**, 121.

2. B. C. Berris, G. H. Hovakeemian, T.-H. Lai, H. Mestdagh and K. P. C. Vollhardt, A New Approach to the construction of Biphenylenes by the Cobalt -Catalyzed Cocyclization of *o*-Diethynylbenzenes with Alkynes. Application to an Iterative Approach to [3]Phenylene, the First member of a Novel Class of Benzocyclobutadienoid Hydrocarbons. *J. Am. Chem. Soc.,* 1985, **107**, 5670–5687.

3. N. H. Pham, S. Parpart, S. Grigoryan, T. N. Ngo, T. T. Dang, T. V. Ghochikyan, A. S. Saghyan, P. Ehlers and P. Langer, Convenient Synthesis of Thieno[3,2-*b*]indoles and Thieno-[3,4-*b*]indoles by Sequential Site-Selective Suzuki and Double C–N Coupling Reactions. *Eur. J. Org. Chem.,* 2017, **3**, 538–550.

4. P. J. Garratt and K. P. C. Vollhardt, Wittig Reactions of 1,2-Benzocyclobutadienequinone. Synthesis of 2-Thianorbiphenylene (Benzo[3,4]cyclobuta[1,2-*c*]thiophene). *J. Am. Chem. Soc*., 1972, **94**, 7087−7092.

5. A. J. Jones, P. J. Garratt and K. P. C. Vollhardt, ^{13}C Shifts in Biphenylene and Analogous Compounds. *Angew. Chem. Int. Ed.,* 1973, **12**, 241−243.

6. S. H. Chanteau and J. M. Tour, Synthesis of Anthropomorphic Molecules: The NanoPutians. *J. Org. Chem.,* 2003, **68**, 8750– 8766.

7. L. Li, J. Xiang and C. Xu, Synthesis of Novel Ladder Bis-Silicon-Bridged *p*-Terphenyls. *Org. Lett.,* 2007, **9**, 4877−4879.

8. L. Dou, J. You, J. Yang, C.-C. Chen, Y. He, S. Murase, T.Moriarty, K. Emery, G. Li and Y. Yang, Tandem Polymer Solar Cells Featuring a Spectrally Matched Low-Bandgap Polymer. *Nat. Photonics,* 2012, **12,** 180–184.

9. P. Deng, L. Liu, S. Ren, H. Li and A. Zhang, N-Acylation: an Effective Method for Reducing the

LUMO Energy Levels of Conjugated Polymers Containing Five Membered Lactam Units. *Chem. Commun.,* 2012, **48**, 6960–6962.

10. M. J. Frisch, G. W. Trucks, H. B. Schlegel, G. E. Scuseria, M. A. Robb, J. R. Cheeseman, G. Scalmani, V. Barone, G. A. Petersson, H. Nakatsuji, X. Li, M. Caricato, A. V. Marenich, J. Bloino, B. G. Janesko, R. Gomperts, B. Mennucci, H. P. Hratchian, J. V. Ortiz, A. F. Izmaylov, J. L. Sonnenberg, D. Williams-Young, F. Ding, F. Lipparini, F. Egidi, J. Goings, B. Peng, A. Petrone, T. Henderson, D. Ranasinghe, V. G. Zakrzewski, J. Gao, N. Rega, G. Zheng, W. Liang, M. Hada, M. Ehara, K. Toyota, R. Fukuda, J. Hasegawa, M. Ishida, T. Nakajima, Y. Honda, O. Kitao, H. Nakai, T. Vreven, K. Throssell, J. A. Montgomery, Jr., J. E. Peralta, F. Ogliaro, M. J. Bearpark, J. J. Heyd, E. N. Brothers, K. N. Kudin, V. N. Staroverov, T. A. Keith, R. Kobayashi, J. Normand, K. Raghavachari, A. P. Rendell, J. C. Burant, S. S. Iyengar, J. Tomasi, M. Cossi, J. M. Millam, M. Klene, C. Adamo, R. Cammi, J. W. Ochterski, R. L. Martin, K. Morokuma, O. Farkas, J. B. Foresman and D. J. Fox, *Gaussian 16*, Revision A.03, Gaussian, Inc., Wallingford CT, 2016.

11. A. D. Becke, Density-Functional Thermochemistry. III. The Role of Exact Exchange. *J. Chem. Phys.*, 1993, **98**, 5648–5652.

12. C. Lee, W. Yang and R. G. Parr, Development of the Colle-Salvetti Correlation-Energy Formula into a Functional of the Electron Density. *Phys. Rev. B*, 1988, **37**, 785–789.

13. S. H. Vosko, L. Wilk and M. Nusair, Accurate Spin-Dependent Electron Liquid Correlation Energies for Local Spin Density Calculations: a Critical Analysis, *Can. J. Phys.*, 1980, **58**, 1200–1211.

14. R. Krishnan, J. S. Binkley, R. Seeger and J. A. Pople, Self-Consistent Molecular Orbital Methods. XX. A Basis Set for Correlated Wave Functions. *J. Chem. Phys.*, 1980, **72**, 650–654.

15. M. M. Francl, W. J. Pietro, W. J. Hehre, J. S. Binkley, M. S. Gordon, D. J. DeFrees and J. A. Pople, Self-Consistent Molecular Orbital Methods. XXIII. A Polarization-Type Basis Set for Second-Row Elements. *J. Chem. Phys.*, 1982, **77**, 3654–3665.

16. M. J. Frisch, J. A. Pople and J. S. Binkley, Self-Consistent Molecular Orbital Methods 25. Supplementary Functions for Gaussian Basis Sets. *J. Chem. Phys*., 1984, **80**, 3265–3269.

17. S. Hashimoto and K. Tahara, Theoretical Study on the Geometry, Aromaticity, and Electronic Properties of Benzo[3,4]cyclobutathiophenes and Their Homologues. *J. Org. Chem.* 2019, **84**, 9850–9858.

18. P. v. R. Schleyer, C. Maerker, A. Dransfeld, H. Jiao and N. J. R. van Eikema Hommes, Nucleus-Independent Chemical Shifts: A Simple and Efficient Aromaticity Probe. *J. Am. Chem. Soc*., 1996, **118**, 6317–6318.

19. F. London, Théorie Quantique Des Courants Interatomiques Dans Les Combinaisons Aromatiques. *J. Phys. Radium,* 1937, **8**, 397–409.

20. H. Fallah-Bagher-Shaidaei, C. S. Wannere, C. Corminboeuf, R. Puchta and P. v. R. Schleyer, Which NICS Aromaticity Index for Planar π Rings Is Best? *Org. Lett.,* 2006, **8**, 863–866.

21. A. Stanger, Nucleus-Independent Chemical Shifts (NICS): Distance Dependence and Revised Criteria for Aromaticity and Antiaromaticity. *J. Org. Chem*., 2006, **71**, 883–893.

22. R. Gershoni-Poranne and A. Stanger, The NICS-*XY*-Scan: Identification of Local and Global Ring Currents in Multi-Ring Systems. *Chem. Eur. J*., 2014, **20,** 5673–5688.

23. R. Gershoni-Poranne and A. Stanger, NICS—nucleus-independent chemical shift in *Aromaticity: Modern Computational Methods and Applications*, ed. I. Fernández, Elsevier, Amsterdam, Netherlands, 2021, pp. 99–154.

24. A. P. Rahalkar and A. Stanger, Aroma Package, https://chemistry.technion.ac.il/en/team/amnon-stanger/

25. J. Jusélius, D. Sundholm and J. Gauss, Calculation of Current Densities Using Gauge-Including Atomic Orbitals. *J. Chem. Phys*., 2004, **121**, 3952–3963.

26. H. Fliegl, S. Taubert, O. Lehtonen and D. Sundholm, The Gauge Including Magnetically Induced

Current Method. *Phys. Chem. Chem. Phys.,* 2011, **13**, 20500–20518.

27. M. Dimitrova and D. Sundholm, Current Density, Current-Density Pathways, and Molecular Aromaticity in *Aromaticity: Modern Computational Methods and Applications*, ed. I. Fernández, Elsevier, Amsterdam, Netherlands, 2021, pp. 155–194.

28. M. Rauhalahti, S. Taubert, D. Sundholm and V. Liégeois, Calculations of Current Densities for Neutral and Doubly Charged Persubstituted Benzenes Using Effective Core Potentials. *Phys. Chem. Chem. Phys.,* 2017, **19**, 7124–7131.

29. U. Ayachit, *The ParaView Guide: A Parallel Visualization Application*, Kitware, Inc., New York, NY, USA, 2015, ISBN 978-1-930934-30-6.

30. T. Lu, and F. Chen, Multiwfn: A Multifunctional Wavefunction Analyzer. *J. Comput. Chem.,* 2012, **33**, 580–592.

31. Rigaku, Crystal Structure 4.3: Crystal Structure Analysis Package, Rigaku Corporation, Tokyo, 2019.

32. G. Sheldrick, A Short History of *SHELX*. *Acta Crystallogr. Sect. A,* 2008, **64**, 112–122.

33. C. F. Macrae, I. Sovago, S. J. Cottrell, P. T. A. Galek, P. McCabe, E. Pidcock, M. Platings, G. P. Shields, J. S. Stevens, M. Towler and P. A. Wood, Mercury 4.0: from visualization to analysis, design and prediction. *J. Appl. Cryst.*, 2020, **53**, 226–235.

34. J. Kruszewski and T. M. Krygowski, Definition of Aromaticity Basing on the Harmonic Oscillator Model. *Tetrahedron Lett.*, 1972, **13**, 3839–3842.

35. T. M. Krygowski, Crystallographic Studies of Inter- and Intramolecular Interactions Reflected in Aromatic Character of π-Electron Systems. *J. Chem. Inf. Comput. Sci.*, 1993, **33**, 70–78.

36. E. R. Johnson, S. Keinan, P. Mori-Sánchez, J. Contreras-García, A. J. Cohen and W. Yang, Revealing Noncovalent Interactions. *J. Am. Chem. Soc.*, 2010, **132**, 6498–6506.

37. S. Grimme, A. Hansen, S. Ehlert and J.-M. Mewes, r^{2}SCAN-3c: A “Swiss Army Knife” Composite

Electronic-Structure Method. *J. Chem. Phys*., 2021, **154**, 064103.

38. J. W. Furness, A. D. Kaplan, J. Ning, J. P. Perdew and J. Sun, Accurate and Numerically Efficient r^2SCAN Meta-Generalized Gradient Approximation. *J. Phys. Chem. Lett*., 2020, **11**, 8208–8215.

39. M. Bursch, J.-M. Mewes, A. Hansen and S. Grimme, Best Practice DFT Protocols for Basic Molecular Computational Chemistry. *Angew. Chem. Int. Ed.,* 2022, **61**, e202205735.

40. E. Caldeweyher, C. Bannwarth and S. Grimme, Extension of the D3 Dispersion Coefficient Model. *J. Chem. Phys*., 2017, **147**, 034112.

41. E. Caldeweyher, S. Ehlert, A. Hansen, H. Neugebauer, S. Spicher, C. Bannwarth and S. Grimme, A Generally Applicable Atomic-charge Dependent London Dispersion Correction. *J. Chem. Phys*., 2019, **150**, 154122.

42. H. Kruse and S. Grimme, A Geometrical Correction for the Inter- and Intra-Molecular Basis Set Superposition Error in Hartree-Fock and Density Functional Theory Calculations for Large Systems. *J. Chem. Phys*., 2012, **136**, 154101.

43. F. Jensen, Basis Sets in *Introduction to Computational Chemistry (3rd edn.)*, John Wiley & Sons, Ltd., West Sussex, UK, 2017, pp. 188–232.

44. A. Schäfer, H. Horn and R. Ahlrichs, Fully Optimized Contracted Gaussian Basis Sets for Atoms Li to Kr. *J. Chem. Phys*., 1992, **97**, 2571–2577.

45. F. Weigend and R. Ahlrichs, Balanced Basis Sets of Split Valence, Triple Zeta Valence and Quadruple Zeta Valence Quality for H to Rn: Design and Assessment of Accuracy. *Phys. Chem. Chem. Phys*., 2005, **7**, 3297–3305.

46. F. Weigend, Accurate Coulomb-Fitting Basis Sets for H to Rn. *Phys. Chem. Chem. Phys.*, 2006, **8**, 1057–1065.

47. F. Neese, The ORCA Program System. *WIREs Comput. Mol. Sci*., 2011, **2**, 73–78.

48. F. Neese, F. Wennmohs, U. Becker and C. Riplinger, The ORCA Quantum Chemistry Program

Package. *J. Chem. Phys*., 2020, **152**, 224108.

49. F. Neese, Software Update: The ORCA Program System—Version 5.0. *WIREs Comput. Mol. Sci*., 2022, **12**, e1606.

50. F. Neese, The SHARK Integral Generation and Digestion System. *J. Comput. Chem.*, 2023, **44**, 381–396.

51. W. Humphrey, A. Dalke and K. Schulten, VMD: Visual Molecular Dynamics. *J. Mol. Graphics,* 196, **14**, 33−38.

52. T. Williams and C. Kelley, Gnuplot 4.5: an Interactive Plotting Program. http://gnuplot.sourceforge.net/

53. K. Senthilkumar, F. C. Grozema, F. M. Bickelhaupt and L. D. A. Siebbeles, Charge Transport in Columnar Stacked Triphenylenes: Effects of Conformational Fluctuations on Charge Transfer Integrals and Site Energies. *J. Chem. Phys*., 2003, **119**, 9809–9817.

54. E. J. Baerends, T. Ziegler, A. J. Atkins, J. Autschbach, O. Baseggio, D. Bashford, A. Bérces, F. M. Bickelhaupt, C. Bo, P. M. Boerrigter, L. Cavallo, C. Daul, D. P. Chong, D. V. Chulhai, L. Deng, R. M. Dickson, J. M. Dieterich, D. E. Ellis, M. van Faassen, L. Fan, T. H. Fischer, C. Fonseca Guerra, M. Franchini, A. Ghysels, A. Giammona, S. J. A. van Gisbergen, A. Goez, A. W. Götz, J. A. Groeneveld, O. V. Gritsenko, M. Grüning, S. Gusarov, F. E. Harris, P. van den Hoek, Z. Hu, C.R. Jacob, H. Jacobsen, L. Jensen, L. Joubert, J. W. Kaminski, G. van Kessel, C. König, F. Kootstra, A. Kovalenko, M. V. Krykunov, E. van Lenthe, D. A. McCormack, A. Michalak, M. Mitoraj, S. M. Morton, J. Neugebauer, V. P. Nicu, L. Noodleman, V. P. Osinga, S. Patchkovskii, M. Pavanello, C. A. Peeples, P. H. T. Philipsen, D. Post, C. C. Pye, H. Ramanantoanina, P. Ramos, W. Ravenek, J. I. Rodríguez, P. Ros, R. Rüger, P. R. T. Schipper, D. Schlüns, H. van Schoot, G. Schreckenbach, J. S. Seldenthuis, M. Seth, J. G. Snijders, M. Solà, M. Stener, M. Swart, D. Swerhone, V. Tognetti, G. te Velde, P. Vernooijs, L. Versluis, L. Visscher, O. Visser, F. Wang, T. A. Wesolowski, E. M. van Wezenbeek, G. Wiesenekker, S. K. Wolff,

T. K. Woo and A. L. Yakovlev, ADF2018, SCM, Theoretical Chemistry, Vrije Universiteit, Amsterdam, The Netherlands, http://www.scm.com.

55. F. M. Bickelhaupt, E. J. Baerends, C. Fonseca Guerra, S. J. A. van Gisbergen, J. G. Snijders, T. Ziegler, Chemistry with ADF. *J. Comput. Chem.,* 2001, **22**, 931.

56. J. P. Perdew, J. A. Chevary, S. H. Vosko, Koblar A. Jackson, Mark R. Pederson, D. J. Singh and C. Fiolhais, Atoms, Molecules, Solids, and Surfaces: Applications of the Generalized Gradient Approximation for Exchange and Correlation. *Phys. Rev. B,* 1992, **46**, 6671.

57. E. V. Lenthe and E. J. Baerends, Optimized Slater-Type Basis Sets for the Elements 1–118. *J. Comput. Chem.*, 2003, **24**, 1142−1156.